

Chemical and isotopic evidence for widespread Eoarchean metasedimentary enclaves in southern West Greenland

Nicole L. Cates^{*}, Stephen J. Mojzsis

Department of Geological Sciences, Center for Astrobiology, University of Colorado, Boulder, CO 80309-0399, USA

Received 18 October 2005; accepted in revised form 3 May 2006

Abstract

New mapping, geochemistry and zircon U–Pb ion microprobe geochronology of pre-3750 Ma rocks from West Greenland was used to identify sedimentary protoliths in a problematic high-grade metamorphic terrane. Samples were collected from southernmost part of the *Itsaq Gneiss Complex* where *Akilia association* supracrustal rocks have previously been noted. Supracrustal lithologies include laterally continuous and variably deformed units of amphibolite, ultramafics and ferruginous quartz–pyroxene rocks. Oxygen isotope and mass-independently fractionated sulfur isotopes, immobile trace elements and rare earth element patterns are consistent with origin of quartz–pyroxene rocks as chemical sediments deposited in a marine hydrothermal setting. We describe a further supracrustal lithology: Garnet-bearing quartz–biotite schists with elevated oxygen isotope values ($\delta^{18}\text{O}_{\text{SMOW}} \geq +16\text{‰}$) and mass-independently fractionated S isotopes consistent with a low-temperature aqueous sedimentary origin. In several enclaves, granitoid gneisses within low-strain limbs transect lithologic contacts and contain inclusions of surrounding rocks. This supports the interpretation that some orthogneisses were originally emplaced as igneous veins that cut supracrustal lithologies. Zircon geochronology on orthogneisses that preserve intrusive relationships confirms minimum ages of *ca.* 3750 Ma for the supracrustals and pooled $[\text{Th}/\text{U}]_{\text{zircon}}$ and $\delta^{18}\text{O}_{\text{zircon}}$ values of older zircon populations are consonant with igneous growth in the bulk composition of the host rocks. Low $[\text{Zr}]_{\text{WR}}$ and high Zr saturation temperatures further minimize the possibility of zircon inheritance. A >3750 Ma age and chemical sedimentary origin for various *Akilia association* lithologies underscores the widespread occurrence of rocks of this kind beyond the type locality on Akilia (island) at the southern limit of the *Itsaq Gneiss Complex*.

© 2006 Published by Elsevier Inc.

1. Introduction

The paucity of a geologic record older than *ca.* 3700 Ma, and the invariably complex metamorphic and deformational histories of ancient terranes, provide dual obstacles to constrain surface conditions on the early Earth. A particularly vexing challenge is to discriminate between competing and often mutually exclusive petrogenetic models for purported Eoarchean (*ca.* 3850–3600 Ma; Bleeker, 2004) sediments *viz.* are they indeed metamorphosed sedimentary rocks or, as proposed by some, the end products of some hybrid meta-igneous or metasomatic process? In strongly deformed and polyphase granitoid gneiss complexes that

surround and intrude the oldest supracrustal enclaves, do the oldest zircon populations represent dominantly original igneous populations, or are they inherited grains? Can rocks of this age preserve isotopic signatures bearing on environmental conditions at the time of life's emergence?

The largest known occurrence of pre-3700 Ma rocks that can confidently be assigned a metamorphic volcano-sedimentary origin—thereby providing data on the nature of early surface environments and life—is located within the geologically and temporally diverse $\sim 3000 \text{ km}^2$ *Itsaq Gneiss Complex (IGC)* in West Greenland (Nutman et al., 1996). The foremost Eoarchean supracrustal assemblage in the IGC is the *Isua supracrustal belt (ISB)* (Moorbath et al., 1973; Bridgwater and McGregor, 1974), which is part of the *Isukasia terrane* of Nutman et al. (1996, 2004). These rocks experienced several episodes of metamorphism culminating in the amphibolite facies (Griffin et al., 1980;

^{*} Corresponding author. Fax: +1 303 492 2606.

E-mail address: nicole.cates@colorado.edu (N.L. Cates).

Rollinson, 2001) with variable degrees of metasomatism (Rose et al., 1996; Rosing et al., 1996) and strain (Nutman, 1984; Myers, 2001). Scattered enclaves of supracrustal rocks locked in pre-3700 Ma gneisses extend from the Inland Ice to coastal and island outcrops, terminating southwards to Føringhavn/Kangerdluarssoruseq (McGregor, 1968, 1973; Black et al., 1971; McGregor and Mason, 1977; McLennan et al., 1984). Early Archean rocks south of Isukasia and Godthåbsfjord compose the *Føringhavn terrane* (Nutman et al., 2004; Friend and Nutman, 2005a,b).

The *Føringhavn terrane* experienced an early (~3650 Ma) episode of granulite facies metamorphism (Griffin et al., 1980) that was regressed to amphibolite facies, with minor exceptions (McGregor and Mason, 1977). Unlike the *Isukasia terrane*, partial melt formation is common in these rocks (Nutman et al., 2000) and they record higher degrees of strain (Myers and Crowley, 2000). As summarized elsewhere (Nutman et al., 1996, 1997, 2004 and references therein) the Nuuk area (Fig. 1) contains numerous <1 to ~100 m enclaves of the *Akilia association* (McGregor and Mason, 1977), conceived by V.R. McGregor as a convenient term for rocks commonly viewed as orphaned members of the same supracrustal assemblage as the *ISB* (personal communication to

S.J.M., July 1997). Supracrustal enclaves in the *IGC* are largely mafic to ultramafic in composition with volumetrically minor (but locally highly variable) amounts of banded iron-formation, quartzite, ferruginous (garnet) biotite schists and rare two-mica schists.

Because the oldest terranes tend to be extensively reworked as a consequence of protracted crustal residence times, assignment of protolith (sedimentary or igneous) to apparent supracrustal assemblages like the *Akilia association* is fraught with difficulty (e.g., Myers and Crowley, 2000). However, field relationships show that the *Akilia association* is present as rafted enclaves in, or intruded by granitoid orthogneisses ranging from tonalitic to dioritic in composition (McGregor, 1979). Debate regarding the age(s) of the compositionally varied and petrogenetically unrelated (McGregor, 2000) “Amîtsoq gneisses” (~3500–3850 Ma) hosting the *Akilia association* has abated somewhat with the implementation of new techniques to differentiate inheritance from primary igneous ages (Mojzsis and Harrison, 2000, 2002a; Krogh et al., 2002; Manning et al., 2006; but see Whitehouse and Kamber, 2005 for an alternative view). The *IGC* gneisses are cut by the ca. 3500 Ma *Ameralik dykes* (McGregor, 1968; Chadwick and Coe, 1983; Nutman et al., 2004). Younger rocks that in some cases encompass the *IGC* include the ~2700 Ma

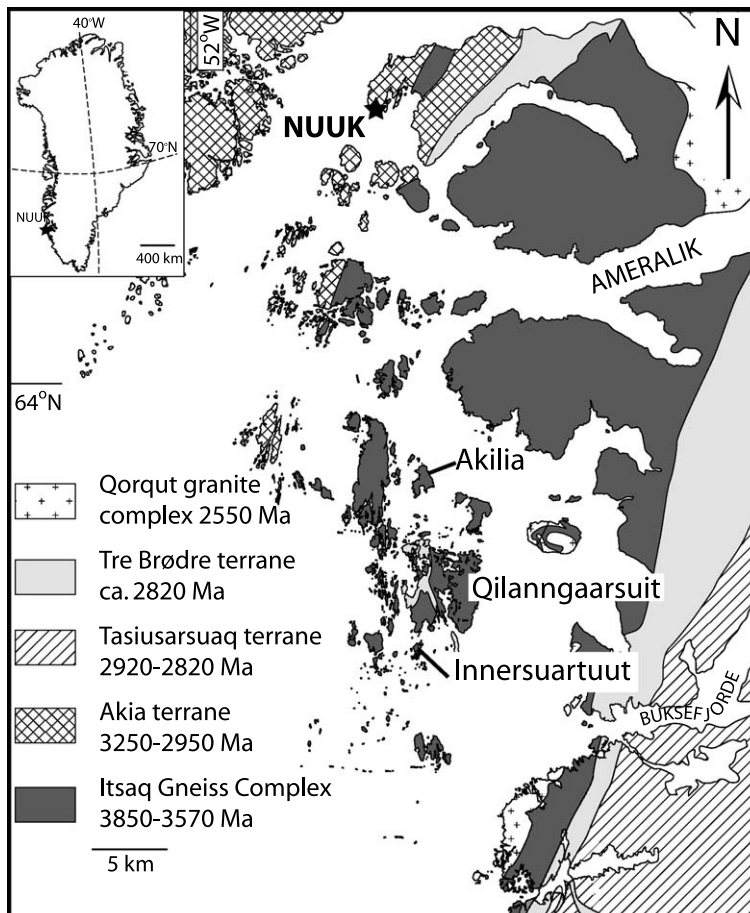


Fig. 1. Geologic domains of West Greenland, south of Nuuk.

Ikkattoq gneisses (Friend et al., 1996) which are tectonically interleaved with the ~2830–2835 Ma *Malene supracrustals* (Nutman et al., 2004). The last major events to affect the terrane were further deformations and retrograde amphibolite metamorphism(s) between 2730 and 2550 Ma (Nutman et al., 2002), emplacement of the post-tectonic *Qorqut Granite Complex* (~2550 Ma) and other late leucogranite/pegmatoid intrusions and thermal events after ~1700 Ma (Pankhurst et al., 1973; Baadsgaard et al., 1976). While details of the post-*Ameralik* history of southern West Greenland are slowly coming to light (e.g., Friend and Nutman, 2005b), it is the geology of the oldest terrane components that remains a subject of vigorous debate.

Current divergence of opinion regarding the geology, age and origin of the Eoarchean rocks of southern West Greenland in general and the *Akilia association* supracrustals in particular can be summarized into four strongly contested interpretations:

- (i) an original sedimentary origin (McGregor and Mason, 1977; McLennan et al., 1984; Nutman et al., 1993, 1997; Mojzsis et al., 1996, 2003a; Mojzsis and Harrison, 2000, 2002b; Anbar et al., 2001; Friend et al., 2002a; Palin, 2002; Dauphas et al., 2004; Nishizawa et al., 2005; Manning et al., 2006) vs. a hybrid meta-igneous/metasomatic origin (Fedo and Whitehouse, 2002a,b; Whitehouse and Fedo, 2002, 2003; Bolhar et al., 2005; Lepland et al., 2005; Whitehouse et al., 2005) for ferruginous (magnetite-rich) banded quartz–pyroxene units in supracrustal enclaves on Akilia (island)—the type locality of the *Akilia association*—and by extension, all rocks of this type;
- (ii) the age and metamorphic history of the oldest orthogneiss components in the vicinity of Akilia (~3500–3850 Ma; Kinny, 1986) established by U–Pb zircon geochronology derived from primary magmatic zircons (Nutman et al., 1996, 1997, 1999, 2002, 2004; McGregor, 2000; Mojzsis and Harrison, 2000, 2002a; Krogh et al., 2002; Manning et al., 2006) or betrayed by widespread contamination from “inherited” zircon incorporated into these rocks from a zircon-rich source (Moorbath et al., 1997; Whitehouse et al., 1999; Kamber and Moorbath, 2000; Kamber et al., 2003; Whitehouse and Kamber, 2005);
- (iii) the likelihood that isotopic signatures bearing on the presence of life (e.g. $\delta^{13}\text{C}$, $\Delta^{33}\text{S}/\delta^{34}\text{S}$, $\delta^{15}\text{N}$ and $\delta^{56}\text{Fe}$) can be preserved in rocks of this antiquity (Schidlowski et al., 1979; Schidlowski, 1988; Mojzsis et al., 1996, 2003a; Rosing, 1999; Mojzsis and Harrison, 2000; Ueno et al., 2002; Dauphas et al., 2004; Nishizawa et al., 2005; Papineau et al., 2005) or the unlikelihood (even declared absence) of such evidence (Myers and Crowley, 2000; Van Zuilen et al., 2002; Fedo and Whitehouse, 2002a; Lepland et al., 2005; Moorbath, 2005a,b; Whitehouse et al., 2005); and

- (iv) the fundamental petrogenetic, structural relationships and crustal growth histories between the *Isukasia* and *F aringhavn* terranes within the *IGC*, i.e., could they be part of a crustal continuum or are they fundamentally separate entities (e.g., Friend and Nutman, 2005a,b)?

Several localities of *Akilia association* supracrustal + orthogneiss enclaves preserve mappable and interpretable primary lithologic contacts at suitable scale to permit direct assessment of the debated interpretations cited above (e.g., Manning et al., 2006). Because so much focus has been placed on the key outcrops at Akilia for which a pre-3830 Ma sedimentary protolith has been proposed and evidence for ancient life has been presented, it makes sense to extend work to other examples of the genre. In an earlier study, Nutman et al. (2002, 2004) reported data—including geological sketch maps and various geochronology data—for several *Akilia association* outcrops south of Akilia. Our study presents new data from three field areas deliberately mapped at high resolution (1:20 to 1:200 scale) to guide detailed sample collection. Field areas were chosen for proximity to the southernmost extent of the *F aringhavn terrane* (Fig. 1) an area that has received far less attention than the northern *Isukasia terrane* (Myers, 2001; and references therein). Care was taken during our mapping to document cross-cutting relationships between orthogneisses and purported supracrustal units, including candidate rocks for geochemical tests of sedimentary protolith.

Our results demonstrate that supracrustal lithologies of the Akilia-type are widespread in the southern *IGC*. If the establishment of continental crust and an evolved rock cycle was an important feature of the Earth since Hadean times (Harrison et al., 2005), the expectation is that yet more relicts of ancient crust will continue to be discovered (Cates and Mojzsis, 2006). This work contributes to determining protolith origins in highly deformed and metamorphosed terranes with applications to a record of surface environments, and life, preserved elsewhere on ancient planetary surfaces.

2. Geology and field relationships of the *Akilia association*

During geologic mapping in the Nuuk region (formerly Godth ab) in the 1960s, it was realized that some mappable gneiss units are characterized by the presence of cross-cutting *Ameralik dikes*, a swarm of amphibolite dikes emplaced in the Archean (McGregor, 1968). As summarized by Nutman and coworkers (1996, 2000, 2002, 2004) these gneisses were informally named “Amitsoq” at the time of their initial description, a term that later became entrenched in the literature to include all Early Archean quartzo-feldspathic units in West Greenland. It is now understood that rather than being a temporally coherent entity, the “Amitsoq gneisses” instead comprise a wide range of lithologies of different ages, origins and

petrogenesis (McGregor, 1979). Unfortunately, the term “Amitsoq” continues to be used to suggest that the gneisses are a more-or-less cogenetic lithologic and chronologic unit occasionally contaminated by older material of unknown origin (Kamber and Moorbath, 2000; Kamber et al., 2003; Whitehouse and Kamber, 2005), which is not the case (e.g., Nutman et al., 1996; McGregor, 2000; Mojzsis and Harrison, 2002a; Manning et al., 2006). A new nomenclature: *Itsaq Gneiss Complex (IGC)* was introduced by Nutman et al. (1996) to emphasize the loose connection of different entities within the same broad structural domain, a terminology that we have adopted for these studies.

The southern *Færinghavn terrane* of the IGC comprises a vast (>1000 km²) and remote milieu. In this study we chose to focus on three specific island localities within the southern part because of the potential for preserving pre-3700 Ma supracrustals had previously been noted in the region.

2.1. Akilia association lithologies

Past fieldwork on the Innersuartaunut and Qilangaarsuit islands was mostly limited to relatively small-scale mapping and sample collection (e.g., Nutman, 1977, unpublished map; Gancarz and Wasserberg, 1977; Gruau et al., 1986; Nutman et al., 1996, 2002). Over the years, brief visits by a number of workers to various island localities south of Nuuk noted small pods and lenses of probable supracrustal rocks in highly deformed gneisses cut by Ameralik dikes. Following previous studies (e.g., McGregor and Mason, 1977; Nutman et al., 1996, 2002) we define *Akilia association* lithologies as mafic amphibolites (*Am*) sometimes with ultramafic inclusions (*Au*); ultramafic pyroxene–amphibole rocks (*Aum*); Fe-rich quartz–pyroxene schists (*Aqp*); various narrow granitoid gneisses (*Ag*) ranging at the scale of a single outcrop from mafic to granodioritic and banded to homogeneous; late leucogranitoids as dikes, sills and pegmatitic veinings (*Lg*); and amphibolitized dikes ascribed to the Ameralik dyke swarm of West Greenland (*Ad*). Other mappable lithologies include leucogabbroic rocks (*Lg*); and a quartz–garnet–amphibole–biotite schist (*Aqg*). Key lithologies are described in detail and whole-rock major-, minor- and trace element analyses are provided in [electronic annex EA-1](#).

To the best of our knowledge, no prior U–Pb ion microprobe zircon geochronology has been carried out on samples from the Innersuartaunut localities explored here and only to a limited extent have they been performed on Qilangaarsuit. It is interesting to note that gabbros from the area of the Innersuartaunut archipelago have yielded the only statistically significant Sm–Nd isochron reported in the *Færinghavn terrane* and define an age of 3887 ± 65 Ma (MSWD: 0.7; Gruau et al., 1986). This observation indicates that ancient crust exists in the vicinity and served as part of the motivation for us to explore this area further.

2.2. Case Study 1: unnamed island west of Innersuartaunut (63°50.2'N, 51°41.5'W)

Innersuartaunut is the collective name for an archipelago of some dozen or so islands located ~38 km directly south of Nuuk, 1.2 km from the SSE point of the big island of Qilangaarsuit and approximately 16 km northwards from the southern boundary of the *Færinghavn terrane* in the Davis Strait. The largest of the islands in the archipelago (~20 km² in area) is referred to in the text as the “main island”. Based on the reconnaissance visits cited above, a candidate supracrustal enclave with excellent exposure was identified on a small island just to the west of the main island.

2.2.1. Geology and structure

The exposure was mapped at 1:200 scale beginning with a 25 × 25 m oriented grid further sub-divided with triangulation points recorded by handheld GPS ($\pm \sim 3$ m). The subdued topography of the outcrops (≤ 5 m) made them ill-suited for topographic mapping. Fig. 2 shows the sampling localities discussed in the text. Lithologic units and contacts were followed as far as the mid-tidal zone where traceable. Supracrustals are well exposed in two places with a total outcrop area of >1000 m². The island rises as two prominences of higher ground on the east and west and the center of the island connecting the two is below high tide. A small skerry ~20 m south is underwater at high tide but connected to the larger outcrop at lowest tide. The supracrustals extend offshore for an unknown distance and there appears to be no exposed contact of the enclaves with the main body of the *Itsaq Gneiss Complex* until one reaches the western shore of the main island, where contacts are complicated by high degree of deformation. It is worthy of note that reconnaissance field studies published in Nutman et al. (2002) and investigated on the ground by us indicate that upwards of 40% of the main island at Innersuartaunut could be made up of supracrustal rocks including well-preserved examples of laminated magnetite-rich BIF that outcrop near the center of the island (GR04063, EA-1).

The northern half of the west prominence of the small island is defined by an isoclinal fold in the quartz–garnet (*Aqg*) rock containing rafts of quartz–pyroxene (*Aqp*) rock which rests above the *Am* unit (Fig. 3A). On the eastern margin of the *Aqg* unit, augen and grey *Ag* gneisses penetrate the unit and may also cross-cut the *Am*–*Aqg* contact, although the contact is obscured by a pegmatite (*Lg*) vein which follows the structural trend of the fold (Fig. 3B). Directly to the south of the nose of the larger fold are a series of smaller tight isoclinal folds within the *Am*, which have a boudinaged *Aqp* raft at their core. Southwards of the *Am* unit is a further unit of *Aqg* with isoclinal folding penetrated by mafic *Ag* gneiss (GR04036) geochemically identical to the one to the north (Fig. 3C). The southwestern end of the island becomes complex structurally, with the mafic gneiss *Am* containing

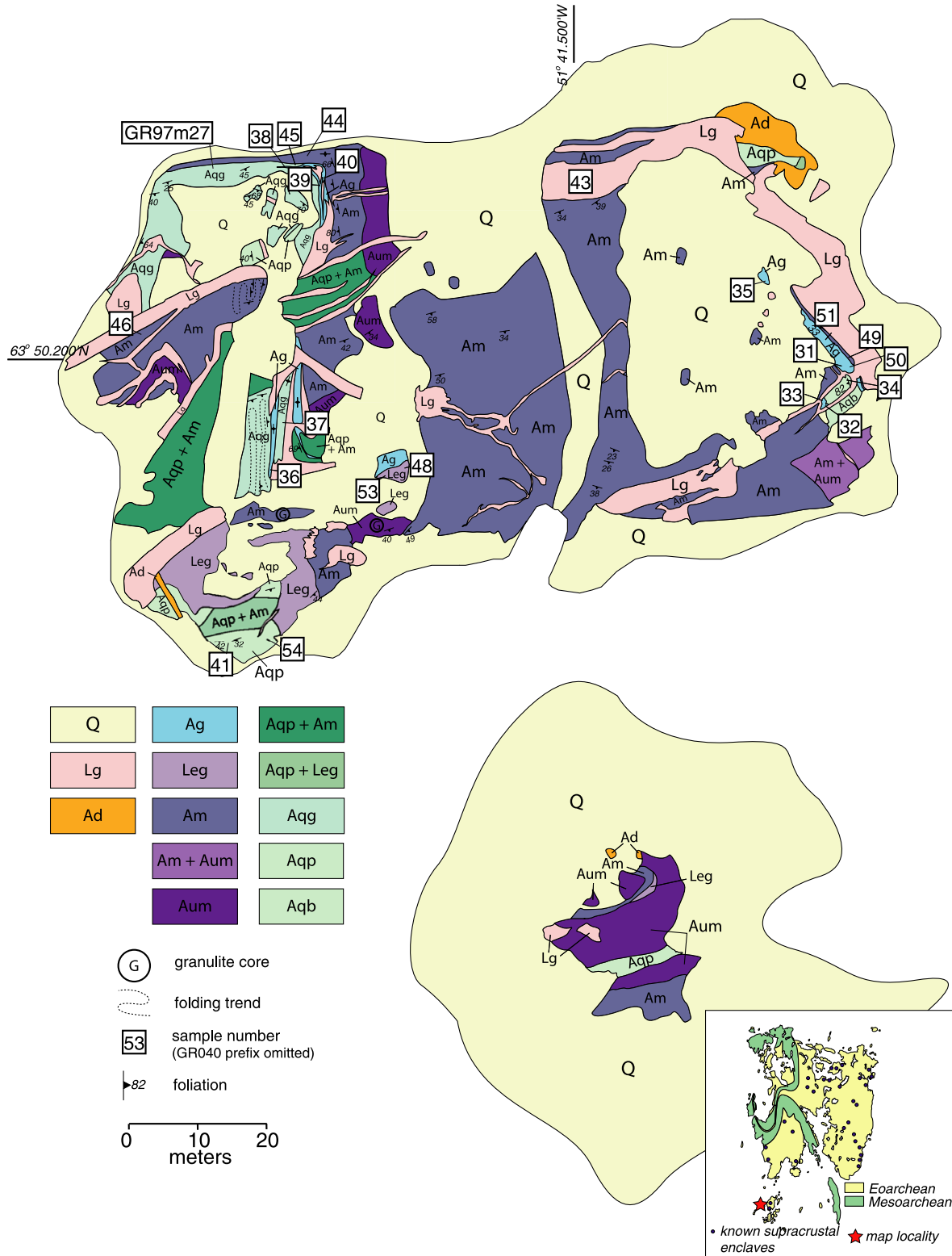


Fig. 2. Geologic map of island west of Innersuartuut (main island). *Q*, Quaternary cover; *Lg*, leucogranite; *Ad*, Amphibolite dike; *Ag*, orthogneisses (undifferentiated IGC); *Leg*, leucogabbro/partial *Am* melt; *Am*, amphibolite; *Aum*, ultramafics; *Aqp*, garnet-bearing quartz-biotite rock; *Aqp*, quartz-pyroxene rock; *Aqb*, quartz-plagioclase-biotite schist.

abundant *Aqp* blocks chaotically arranged on a small scale (<1 m) and weakly foliated to massive. At the south-western point, an east-west foliation dominates the outcrop shared by leucogabbro (*Leg*) and mafic gneiss

(*Am*) and a large block of *Aqp* that repeats the same sense of foliation. The east-west foliation continues in the *Am* unit across the low-standing center of the island and is traceable to the eastern shore. North-south foliation on

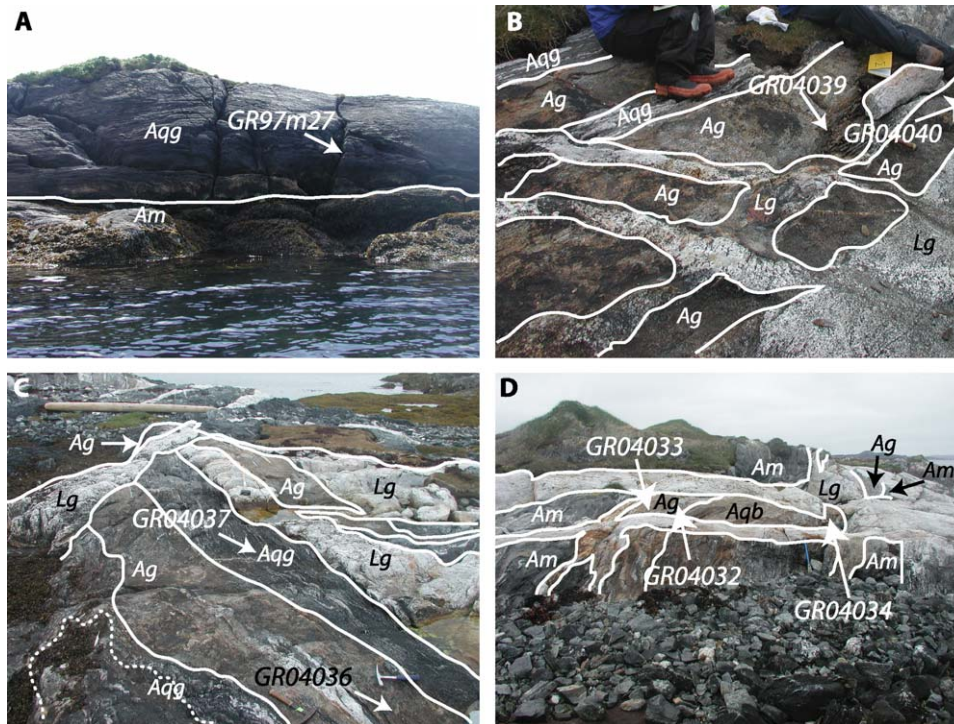


Fig. 3. Field photographs of key contact relationships from the mapped island west of Innersuaartuut. (A) Large unit of garnet-bearing quartz-biotite rock (*Aqq*) overlying amphibolite (*Am*). (B) Intrusive relationship of orthogneisses (*Ag*) with garnet-quartz-biotite rock (*Aqq*) and amphibolite (*Am*) partly obscured by pegmatite (*Lg*). (C) Garnet-bearing quartz-biotite rock (*Aqq*) penetrated by orthogneiss (*Ag*). (D) Amphibolite (*Am*) cross-cut by orthogneiss (*Ag*) from the SE of the island. Sample locations are shown.

the east is sympathetic to the northwestern corner of the island. Here, a small outcrop of quartz-plagioclase-biotite schist (*Aqb*, GR04034) and the *Am* unit are intruded by a series of *Ag* sheets (GR04031, GR04032, GR03033, GR04050, and GR04051; EA-1) that are chemically distinct from those on the western half of the island (Fig. 3D). A package of small (<1 m wide) *Ag* sheets can be traced along strike for several meters into small exposures in the cover, but is eventually lost and does not reemerge on the north shore, which is dominated by late leucogranites (*Lg*). The small skerry to the south of the main outcrop is dominantly *Am* containing a raft of *Aqp* rock with east-west foliation defined by alternating quartz- and pyroxene-rich bands sandwiched between mafic gneisses near the center of the skerry.

2.2.2. Quartzo-feldspathic sheets in the map area

Contacts between datable *Ag* gneisses and *Akilia association* supracrustal enclaves are vital to understanding the age and origin of these bodies. If orthogneisses and supracrustal lithologies are tectonically interleaved during deformation rather than intrusive, the ages of the orthogneisses are not relevant to the minimum age of the enclave. In any high-grade metamorphic terrane that hosts potential volcano-sedimentary enclaves only detailed large-scale mapping used to guide sample collection for geochemistry and geochronology can resolve this issue, as exemplified by past debates over the *Akilia* island locality.

2.3. Case Study 2: SE Qilanngaarsuit

Based on previous work by Nutman et al. (2002) that builds on earlier studies (McGregor and Mason, 1977; Chadwick and Coe, 1984; McLennan et al., 1984; Nutman, 1984; Nutman et al., 1996, 2000), several dominantly ultramafic supracrustal enclaves were noted on the southeastern margin of Qilanngaarsuit (Fig. 1). During our summer 2004 field work, one of these outcrops was located, mapped and sampled. Although GPS coordinates of our map area correspond with “locality 4” in Nutman et al. (2002), the outcrop most resembles their “locality 7” described as “peridotites...intruded and broken-up by anastomosing sheets of dark grey and leucocratic orthogneiss”. Partly based on this ambiguity in terms of sample description, precise location of the outcrop, mapping and geochronology, as well as the potential for additional lithologies to those described in Nutman et al. (2002) such as the garnet-biotite schist unit described in EA-1 (*Agb*), this location was selected as a study target.

2.3.1. Geology and structure

The outcrop was mapped at 1:100 m scale (Fig. 4) using a 15 × 25 m oriented grid with triangulation points recorded by handheld GPS ($\pm \sim 3$ m). The rocks are largely ultramafic in composition enclosed on all sides by gneisses. The overall structural trend is defined by a strong NE-SW foliation, moderately to steeply dipping (~ 45 – 70°) to the

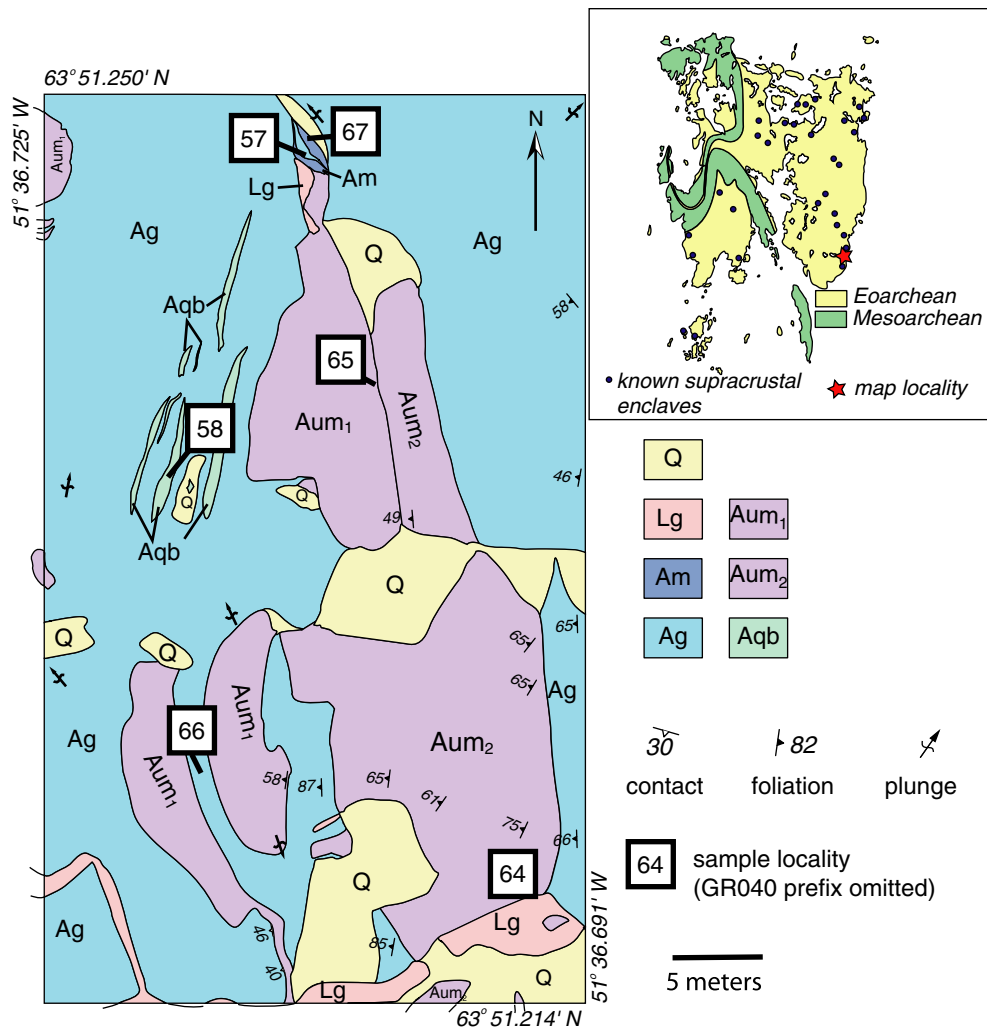


Fig. 4. Geologic map of outcrop from SE Qilannaarsuit. *Q*, Quaternary cover; *Lg*, leucogranite; *Am*, amphibolite; *Ag*, orthogneisses (undifferentiated IGC); *Aum*₁, hornblendite; *Aum*₂, Anthophyllite schist; *Aqb*, quartz-biotite schist.

west and plunging northward. The outcrop pattern is defined by a series of four ultramafic lobes rafted within *Ag*. Ultramafic units have different lithologies: an anthophyllite schist dominates the east and is in sharp contact with hornblendite to the west (EA-1) which do not appear to cross-cut one another. Neighboring tonalitic gneisses enclose a suite of thin, rusty colored units of garnet-biotite-anthophyllite schist (*Agb*) parallel to foliation. At the northernmost extent of the outcrop, an amphibolite (*Am*) and grey gneiss unit are infolded into a hornblendite unit.

2.4. Case Study 3: Western Innersuartaunut

On the western shore of the main island of Innersuartaunut directly across a channel from Case Study #1, an approximately 3-m-wide outcrop of ferruginous quartzite (*Aqp*) + amphibolite (*Am*) is repeatedly disrupted by sheets of tonalitic orthogneiss and a paragneiss. Based on the recognized cross-cutting relationships, this location was selected as a study target during reconnaissance sampling (63°50.379'N51°41'25.5"W).

2.4.1. Geology and structure

The outcrop was mapped at a 1:20 m scale using a 2 × 2 m grid with a corner point recorded by handheld GPS ($\pm \sim 3$ m) and corrected using field photographs. Fig. 5 shows the sampling localities discussed herein. The dominant lithotypes are banded (grey) tonalitic orthogneisses (*Ag*), ferruginous quartz-pyroxene schists (*Aqp*), late leucogranitoids as dikes, sills and pegmatitic veinings (*Lg*) and a minor body (several cm wide) of mafic amphibolite (*Am*). The center and northern edge of the outcrop preserves small rafts of quartz-pyroxene (*Aqp*) rock floating in the gneisses. At the top of the field photo in Fig. 5 grey gneisses penetrate and disrupt the *Aqp* unit and in several areas the contact is partially obscured by a pegmatite (*Lg*) vein. The various *Ag* units record a strong foliation on a small scale (<1 m) and are of varying composition (*GR0081*, *GR0082*, and *GR0083*; EA-1). The suite of narrow (<1 m) *Ag* sheets that build this outcrop can be traced for several meters, but are eventually lost to the chaotic mass of highly deformed gneisses that dominates the area.

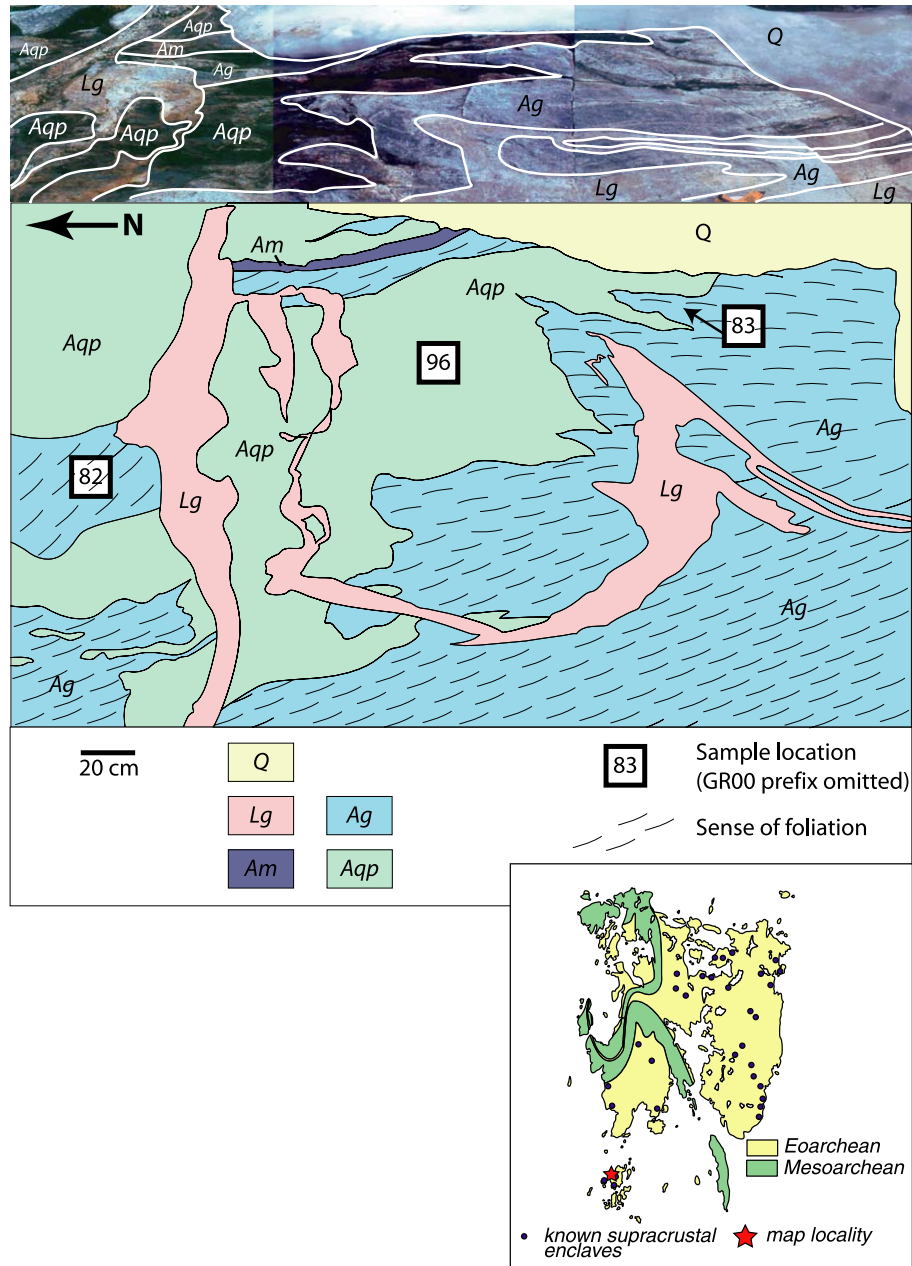


Fig. 5. Geologic map of outcrop from western shore of main island of Innersuartuut with annotated field photomosaic. *Q*, Quaternary cover; *Lg*, leucogranite; *Am*, amphibolite; *Ag*, orthogneisses (undifferentiated IGC); *Aqp*, quartz-pyroxene rock.

3. Analytical techniques

Samples collected for analysis were separated into two categories: those earmarked for whole-rock major-, minor-, trace element and stable isotope geochemical characterizations and a subset of quartzo-feldspathic gneisses and biotite schists chosen based on field relations and mineralogy for detailed geochronological analysis. Granitoid gneiss samples were selected for study based on potential intrusive relationships with supracrustal rocks.

3.1. Sample preparation methods

Freshly broken and unweathered (when possible) samples were divided into three lots: (a) archival samples; (b) chips cut by diamond saws for thin section work; and (c) sample powders for geochemistry and zircon separation. Rocks for powders were initially hand-divided, crushed in large

agate or steel mortars and powdered in a tungsten-carbide shatter box. Homogenized splits from whole-rock powders were prepared for geochemical analysis at ANU-PRISE (Canberra, Australia) and the University of Tasmania. Powder splits of selected samples were separated into whole-rock, magnetite and quartz fractions for oxygen isotope analyses at the Laboratoire de géochimie isotopique (Université Laval, Québec).

Powder splits of samples for combined zircon geochronology and *in situ* zircon oxygen isotope measurements were sieved at $\leq 400 \mu\text{m}$, processed through heavy liquids, cleaned in acetone and subsequently passed through a Franz magnetic separator following our usual procedures (Mojzsis et al., 2003b). Zircon yields were highly variable depending on the rock type (see EA-1). Grains from the least magnetic fraction were handpicked under a binocular microscope, placed on adhesive tape, cast in Buehler[®] epoxide resin with standard zircon AS3 (Paces and Miller, 1993; Black et al., 2003) and polished in stages to $0.25 \mu\text{m}$ alumina until grain centers were reached. Zircons were characterized by optical (transmitted

and reflected light), back-scattered electron microscopy (BSE) and cathodoluminescence (CL) imaging. Prior to ion microprobe analysis, grain mounts were cleaned in 1 N HCl solution to reduce common Pb contamination, rinsed in ultrapure water and dried in air.

Sample chips with visible sulfides were set aside for *in situ* multiple sulfur isotope ($\delta^{34}\text{S}/\Delta^{33}\text{S}$) thin section analyses by multicollector ion microprobe and prepared using standard petrographic techniques. The incidence of sulfides in individual samples was mapped in reflected light microscopy and the phases characterized by electron microprobe (Greenwood et al., 2000; Mojzsis et al., 2003a; Papineau et al., 2005). In cases where sulfide grains were only present near the edge of the thin section, the glass slides were divided by a small diamond saw around the sulfide region(s) and re-cast with sulfide standards and polished to 0.25 μm alumina in alcohol, cleaned and Au-coated.

3.2. Ion microprobe U–Pb zircon geochronology

Prior to conventional U–Pb analysis described below, preliminary results for zircons separated from samples from Case Study 3 were obtained using the ANU SHRIMP-II in Pb-isotope multicollector mode for ^{204}Pb – ^{206}Pb – ^{207}Pb – ^{208}Pb in a rapid (6 s/analysis) survey of several dozen zircons to confirm that gneisses were Eoarchean, a technique more fully described in Turner et al. (2004).

All conventional U–Pb zircon geochronology was determined using the UCLA CAMECA *ims1270* high-resolution ion microprobe under routine conditions (e.g., Mojzsis and Harrison, 2002a; Mojzsis et al., 2003b); a short summary is provided. The standard operating conditions for U–Pb analyses were a ~ 6 nA O_2^- primary beam focused to a 25 μm spot; the ion microprobe was operated at a mass-resolving power of ~ 6000 . Oxygen flooding to a pressure of 3.5×10^{-5} torr was employed to increase Pb^+ yields (Schuhmacher et al., 1994). Zircon ages for our unknowns were determined by comparison with a working curve defined by multiple measurements of standard AS3 that yields concordant $^{206}\text{Pb}/^{238}\text{U}$ and $^{207}\text{Pb}/^{235}\text{U}$ ages of 1099.1 ± 0.5 Ma (Paces and Miller, 1993; Black et al., 2003). A summary of the geochronology is presented in Table 1 and all data are reported in electronic annex EA-2.

3.3. Ion microprobe multicollector sulfur isotope analysis of sulfides

All sulfides analyzed in this work were measured for their multiple sulfur isotopes (^{32}S , ^{33}S , ^{34}S) on adjacent Faraday detectors in multicollection mode using the UCLA Cameca *ims1270* ion microprobe. Instrumental methods are described elsewhere (Mojzsis et al., 2003a; Papineau et al., 2005) and a short summary is provided here. A liquid nitrogen cold finger was used in the sample chamber to lower the partial pressure of water vapor and thus decrease the contribution of the isobar $^{32}\text{SH}^-$ to $^{33}\text{S}^-$. Mean times per analysis were ~ 360 s, composed of 200 s of pre-sputtering; 15 cycles of data acquisition at 10 s per cycle; and ~ 120 s setup time between analyses for a total acquisition time of ~ 8 min per analysis spot. Secondary-ion beam intensities were approximately 10^9 , 10^7 , and 5×10^7 ions per second for $^{32}\text{S}^-$, $^{33}\text{S}^-$, and $^{34}\text{S}^-$, respectively, at a mass-resolving power of ~ 5000 . Multiple analyses on seven sulfide standards containing pyrite, pyrrhotite, chalcopyrite and troilite were performed on sulfide standard mount *GM4* to correct for instrumental mass fractionation. The measurements have external errors, described as the reproducibility of the standards (electronic annex EA-3) excluding CDT at 2σ and taking into account the reproducibility of the detector baselines, of $\pm 0.66\%$ for $\delta^{34}\text{S}$, $\pm 0.36\%$ for $\delta^{33}\text{S}$ and $\pm 0.096\%$ for $\Delta^{33}\text{S}$. Further details of our $\Delta^{33}\text{S}$ data reduction and standards are presented in Papineau et al. (2005). Reported $\Delta^{33}\text{S}$ values were calculated using the formula $\Delta^{33}\text{S} = 1000 \cdot [(1 + \delta^{33}\text{S}/1000) - (1 + \delta^{34}\text{S}/1000)^{0.518}]$ and uncertainties in our sulfur isotope data are at the 2σ level (Table 2).

3.4. Ion microprobe multicollector oxygen isotope analysis of zircon

Following the procedures of Mojzsis et al. (2001) we used the UCLA *ims1270* ion microprobe in multicollector mode to obtain precise oxygen

isotope compositions of individual zircons from granitoid orthogneisses and rocks targeted for sedimentary protolith studies; a brief summary of the analytical conditions is given here. Following detailed U–Pb geochronology, target zircons were photographed to locate existing ion microprobe pits, re-polished until all previous spots were removed, cleaned, and gold-coated. Simultaneous measurements of $^{16}\text{O}^-$ and $^{18}\text{O}^-$ secondary-ion beams were made on adjacent Faraday collectors using a ~ 6 nA Cs^+ primary ion beam focused to a 25 μm diameter spot. A liquid nitrogen cold finger was used to scavenge water and CO_2 from the analysis chamber and a mass-resolving power of ~ 2000 was sufficient to separate $^{18}\text{O}^-$ and $^{16}\text{O}^-$ from molecular interferences. Typical count rates were 2×10^9 for $^{16}\text{O}^-$ and 4×10^6 for $^{18}\text{O}^-$ and the total integration time per analysis was approximately 360 s. Instrumental mass fractionation (IMF) was corrected using standard zircon (electronic annex EA-4) AS3 ($\delta^{18}\text{O} = 5.34 \pm 0.03\%$; unpublished data). Uncertainties in our oxygen isotope data for zircon in Table 3 are reported at the 1σ level.

4. Zircon U–Pb geochronology

4.1. Case Study 1: Island west of Innersuartuut

Bodies of *Ag* orthogneisses within the supracrustal enclaves all occur as narrow sheets or veins that follow the local deformation patterns. Because of the strong deformation, cross-cutting relationships are rarely preserved, but field observations at the appropriate scale permit some to be identified. Where such relationships exist, they have been noted in the text and maps.

Nine orthogneiss (*Ag*) samples were chosen for geochronology. The samples range from typical TTG compositions (mostly granodiorite) to mafic and, at the opposite end of the spectrum, quartz monzodiorite (*EA-1*). Zirconium contents are almost all low with $[\text{Zr}]$ typically less than 100 ppm, and corresponding zircon saturation temperatures of 640–740 $^\circ\text{C}$, which place them near the H_2O -saturated temperature of TTG melt formation (Wyllie et al., 1997) and therefore the large-scale preservation of inherited zircons is not likely (Watson, 1996).

Zircon morphologies for all *Ag* units are relatively consistent; most grains are clear to pink, 70–150 μm in length, with high aspect ratios and rounded tips. When viewed by CL, some grains show well-developed oscillatory zoning at their cores with poorly zoned rims, although this relationship is not universal. All CL images are available in electronic annex EA-5.

Four samples of candidate sedimentary rocks were selected to test for the presence of detrital grains and metamorphic zircon growth. Zircons in these samples were rare, mostly small and rounded and with very little zoning.

4.1.1. Eastern *Ag* units ($N63^\circ 50' 12''$ $W51^\circ 41' 28''$)

Sample *GR04051* is a grey orthogneiss from package of *Ag* units and cross-cuts and contains pieces of the amphibolite unit (*Am*) to the west (Fig. 2). Zircons from *GR04051* record five distinct events (Fig. 6A), the oldest of which is assigned a magmatic origin with a weighted mean age of 3724 ± 10 Ma (MSWD = 0.86) and a tightly grouped population of igneous-like $[\text{Th}/\text{U}]_{\text{Zr}}$ values (0.62 ± 0.09 ; see Hoskin and Schaltegger, 2003 for a discussion on expected

Table 1
Zircon geochronology summary for selected samples

Eastern shore of island west of Innersuartaat.

population		I	II	III	IV	V	VI	VII
GR04051	age ($^{207}\text{Pb}/^{206}\text{Pb}$) ¹	3724±10*		3579±9*	3495±9*	3389±28*		
	MSWD ²	0.86		2.3	1.11	1.9		
	[Th/U] _{zr} ³	0.62±0.09		0.48±0.40	0.21±0.13	0.22±0.17		
	n ⁴			7	4	3		
GR04032	age ($^{207}\text{Pb}/^{206}\text{Pb}$)		3677±13	3552±10*		3334 ⁺⁶⁸ ₋₃₁	3037 ⁺³³ ₋₂₉	2697±50
	MSWD		-	0.44		-	0.33	2.6
	[Th/U] _{zr}		1.06	0.52±0.04		0.52±0.03	0.16±0.10	0.35±0.04
	n		1	3		2	4	3
GR04031	age ($^{207}\text{Pb}/^{206}\text{Pb}$)	3693±19*	3627 ⁺²⁷ ₋₁₈	3555 ⁺¹⁶ ₋₂₀	3467 ⁺²⁴ ₋₂₅			
	MSWD	1.1	0.46	0.2	1.7			
	[Th/U] _{zr}	0.40±0.06	0.51±0.26	0.23±0.15	0.17±0.09			
	n	4	8	8	3			
GR04035	age ($^{207}\text{Pb}/^{206}\text{Pb}$)	3701±15	3649 ⁺²² ₋₂₀	3555±29				
	MSWD	0.6	1.01	4.9				
	[Th/U] _{zr}	0.66±0.29	0.39±0.13	0.085±0.13				
	n	5	4	11				

Qilangaarsuit.

population		I	II	III	IV	V	VI	VII
GR04066	age ($^{207}\text{Pb}/^{206}\text{Pb}$)		3671 ⁺³⁸ ₋₃₅					2713±30*
	MSWD		0.86					0.29
	[Th/U] _{zr}		0.45±0.11					0.36±0.20
	n		3					6
GR04057	age ($^{207}\text{Pb}/^{206}\text{Pb}$)		3680 ⁺⁶⁰ ₋₅₄					2715±13*
	MSWD		0.97					2.3
	[Th/U] _{zr}		0.48±0.17					0.22±0.08
	n		4					6
GR04058	age ($^{207}\text{Pb}/^{206}\text{Pb}$)		3619±67					
	MSWD		3.75					
	[Th/U] _{zr}		0.43±0.14					
	n		15					

¹Ages reported as isochron intercept age unless indicated by a *, in which case age is the weighted mean.

²Mean standard weight of the deviates.

³Average Th/U of zircons in population.

⁴Number of analyses.

Western shore of island west of Innersuartaat.

population		I	II	III	IV	V	VI	VII
GR04036	age ($^{207}\text{Pb}/^{206}\text{Pb}$)	3755±12*	3637 ⁺²³ ₋₁₉			3282±15*		
	MSWD	-	1.11			-		
	[Th/U] _{zr}	0.38±0.01	1.41±1.10			0.53±0.01		
	n	1	5			1		
GR04039	age ($^{207}\text{Pb}/^{206}\text{Pb}$)	3687±12*	3623±12*	3519±10*		3406 ⁺⁴⁵ ₋₁₉		
	MSWD	-	1.2	2.4		0.77		
	[Th/U] _{zr}	0.74±0.02	2.3±2.5	2.0±2.7		1.6±2.5		
	n	1	5	5		8		
GR04037	age ($^{207}\text{Pb}/^{206}\text{Pb}$)		3632±16*					2702±30*
	MSWD		1.1					0.81
	[Th/U] _{zr}		0.04±0.02					0.08±0.10
	n		3					4
GR97m27	age ($^{207}\text{Pb}/^{206}\text{Pb}$)		3642±15*	3590±8*		3320±22*		2690±38*
	MSWD		2.5	1.9		-		0.31
	[Th/U] _{zr}		0.20±0.18	0.15±0.11		0.14±0.07		0.21±0.08
	n		6	13		2		8

Innersuartaat (main island).

population		I	II	III	IV	V	VI	VII
GR0081	age ($^{207}\text{Pb}/^{206}\text{Pb}$)		3594±6*	3535±9	3467±21			2869±16*
	MSWD		-	0.15	5.8			-
	[Th/U] _{zr}		0.46±0.01	0.36±0.09	0.16±0.12			0.22±0.01
	n		1	3	5			1
GR0082	age ($^{207}\text{Pb}/^{206}\text{Pb}$)		3629±7	3586±8	3518±5			
	MSWD		1.2	0.32	-			
	[Th/U] _{zr}		0.53±0.10	0.40±0.17	0.45±0.01			
	n		5	4	1			
GR0083	age ($^{207}\text{Pb}/^{206}\text{Pb}$)		3617±34*	3548±13*	3428±9*			
	MSWD		6.1	2.9	-			
	[Th/U] _{zr}		0.66±0.4	0.48±0.2	0.28±0.01			
	n		3	6	1			

Table 2
Sulfur isotopic data

Analysis name	Phase	$^{32}\text{S} \times 10^8$ (cps)	$\delta^{34}\text{S}_{\text{CDT}}$	Internal $\pm 1\sigma$	External $\pm 2\sigma$	$\delta^{33}\text{S}_{\text{CDT}}$	Internal $\pm 1\sigma$	External $\pm 2\sigma$	$\Delta^{33}\text{S}$	Internal $\pm 1\sigma$	External $\pm 2\sigma$
<i>Session 1</i>											
GR04054b_1	po	4.013	2.15	0.03	1.09	3.01	0.09	0.67	1.90	0.09	0.25
GR04054d_1	po	3.989	2.22	0.03	1.09	3.10	0.08	0.67	1.95	0.08	0.24
GR04054e_1	po	4.178	2.17	0.02	1.09	3.11	0.07	0.66	1.99	0.07	0.24
GR04041b_1	po	4.648	1.67	0.03	1.09	3.51	0.08	0.67	2.64	0.08	0.24
GR04041c_1	po	1.934	0.62	0.06	1.09	3.46	0.19	0.75	3.14	0.19	0.42
GR04041a_1	po	3.553	3.07	0.02	1.09	4.18	0.12	0.69	2.59	0.12	0.30
GR04041d_1	po	3.414	0.72	0.03	1.09	3.15	0.09	0.67	2.78	0.09	0.25
GR04041e_1	po	3.806	1.76	0.03	1.09	4.06	0.09	0.67	3.15	0.09	0.25
<i>Session B</i>											
GR0096c_1	po	8.430	0.97	0.03	1.04	0.73	0.06	0.58	0.23	0.06	0.19
GR0096d_1	po	8.646	1.24	0.02	1.04	0.92	0.05	0.58	0.27	0.05	0.18
GR0096b_1	po	8.368	1.68	0.02	1.04	1.05	0.04	0.57	0.18	0.04	0.18
GR0096a_1	po	4.182	1.75	0.03	1.04	1.36	0.09	0.60	0.45	0.09	0.24
GR04063f_1	po	10.31	1.75	0.03	1.04	2.25	0.04	0.57	1.35	0.04	0.17
GR04063e_1	po	7.424	0.51	0.02	1.04	1.75	0.05	0.58	1.49	0.05	0.19
GR04063b_1	po	9.941	1.15	0.03	1.04	1.92	0.05	0.57	1.33	0.05	0.18
GR04063b_2	po	9.716	0.69	0.02	1.04	1.68	0.05	0.58	1.32	0.05	0.19
GR04063a_1	po	9.225	1.47	0.02	1.04	2.07	0.05	0.58	1.31	0.05	0.19
<i>Session 2004</i>											
GR97m27_1_1	po	5.257	0.97	0.04	0.90	1.18	0.07	0.49	0.68	0.06	0.12
GR97m27_1_2	po	6.294	0.18	0.02	0.90	0.89	0.06	0.49	0.80	0.06	0.12
GR97m27_2_1	po	6.902	-0.43	0.02	0.90	0.49	0.05	0.49	0.71	0.06	0.12
GR97m27_2_2	po	6.074	-0.91	0.02	0.90	0.50	0.06	0.49	0.98	0.06	0.12
GR97m27_3_2_1	po	6.877	-0.08	0.03	0.90	0.81	0.06	0.49	0.84	0.05	0.11
GR97m27_3_2_2	po	6.982	0.43	0.02	0.90	0.93	0.05	0.49	0.70	0.05	0.10
GR97m27_3_2_3	po	5.438	0.84	0.02	0.90	1.23	0.07	0.50	0.80	0.08	0.15
GR97m27_3_1_1	po	4.184	0.64	0.05	0.90	1.20	0.06	0.49	0.87	0.06	0.12
GR97m27_3_1_2	po	6.204	0.26	0.02	0.90	0.93	0.05	0.49	0.80	0.05	0.10
GR97m27_3_1_3	po	7.880	0.11	0.02	0.90	0.78	0.04	0.48	0.72	0.05	0.09
GR97m27_3_1_4	po	5.910	0.98	0.03	0.90	1.18	0.09	0.51	0.67	0.09	0.17
GR97m27_3_3_1	po	7.099	-1.31	0.06	0.90	0.00	0.06	0.49	0.68	0.05	0.09
GR97m27_3_3_2	po	6.118	0.29	0.02	0.90	0.93	0.06	0.49	0.78	0.06	0.11
GR97m27_5_1	po	8.124	-1.10	0.02	0.90	0.17	0.04	0.48	0.75	0.04	0.09
GR97m27_6_1	po	4.906	-1.50	0.04	0.90	0.01	0.04	0.48	0.79	0.04	0.08
GR97m27_6_2	po	4.183	-1.81	0.05	0.90	-0.11	0.09	0.51	0.83	0.09	0.18
GR97m27_9_1	po	2.975	0.24	0.03	0.90	0.79	0.10	0.52	0.67	0.11	0.21
GR97m27_7_1	po	7.627	0.02	0.03	0.90	0.84	0.05	0.49	0.83	0.06	0.12
GR97m27_9_2	po	2.960	-1.16	0.03	0.90	0.13	0.16	0.58	0.72	0.17	0.34
GR97m27_9_3	po	4.342	-1.29	0.04	0.90	0.03	0.05	0.49	0.70	0.05	0.10
GR97m27_9_4	po	6.467	0.86	0.03	0.90	1.25	0.08	0.50	0.80	0.08	0.16
GR97m27_9_5	po	6.582	-0.65	0.03	0.90	0.51	0.05	0.49	0.85	0.05	0.10

po, pyrrhotite.

Th/U values in igneous vs. metamorphic zircons) relative to the younger populations (Table 1).

All grains from the oldest population have cores with strong oscillatory zoning and poorly zoned rims in CL (EA-5). This is in stark contrast with the second (younger) population which is equally well defined based on U–Pb geochronology with a weighted mean of 3579 ± 9 Ma (Table 1) where two >96% concordant grains (8_1 and 17_1, EA-5) have very different morphologies: One is from a core with oscillatory zoning and one is from an unzoned tip. Additionally, $[\text{Th}/\text{U}]_{\text{Zr}}$ from the dark tip is typical of metamorphic zircon (0.097) whereas the zoned core has a $[\text{Th}/\text{U}]_{\text{Zr}}$ indistinguishable from igneous zircons (0.641). The seven analyses which define the second population

are from zircons that display a variety of morphologies in CL: (i) dark, unzoned cores; (ii) zoned cores with thin overgrowths; (iii) zoned cores with large overgrowths; and (iv) large overgrowth. The different morphologies are also accompanied by highly variable $[\text{Th}/\text{U}]_{\text{Zr}}$ (0.097–1.05).

These observations support the interpretation that the younger population of zircons is metamorphic and that the oscillatory zoning is an inherited texture (ghost texture; Hoskin and Schaltegger, 2003 and references therein) from a primary magmatic zircon that has undergone solid-state recrystallization. Grains from the second age population with ghost oscillatory zoning preserve magmatic $[\text{Th}/\text{U}]_{\text{Zr}}$, as do those with much younger ages (12_1 and 13_1; 3485 ± 12 Ma and 3235 ± 19 Ma, respectively). This

Table 3
Zircon oxygen isotopic data

Name	¹⁸ O Counts	¹⁶ O Counts	$\delta^{18}\text{O}_{\text{zircon}}^a$ Corrected 1σ
<i>Mount GRIN_1</i>			
GR0083_33_1	4.10E+06	2.03E+09	8.77 ^f ± 0.08
GR0083_33_2	4.02E+06	1.99E+09	8.94 ^f ± 0.07
GR0083_12_1	4.14E+06	2.05E+09	6.91 ^c ± 0.06
GR0083_12_2	4.16E+06	2.06E+09	8.33 ^f ± 0.09
GR0083_12_3	4.20E+06	2.08E+09	8.52 ^f ± 0.06
GR0082_12_1	4.04E+06	2.00E+09	8.66 ^c ± 0.06
GR0082_12_2	4.14E+06	2.05E+09	8.63 ^c ± 0.06
GR0082_12_3	4.11E+06	2.03E+09	8.63 ^c ± 0.06
GR0082_20_1	4.11E+06	2.04E+09	4.92 ^f ± 0.06
GR0082_20_2	4.08E+06	2.03E+09	5.91 ^f ± 0.06
GR0082_10_1	4.06E+06	2.02E+09	4.65 ^c ± 0.09
GR0082_10_2	4.12E+06	2.05E+09	6.01 ^c ± 0.08
GR0082_10_3	4.18E+06	2.07E+09	6.18 ^c ± 0.07
GR0082_10_4	4.09E+06	2.03E+09	4.19 ^f ± 0.06
GR0082_8_1	4.13E+06	2.05E+09	5.48 ^f ± 0.06
GR0082_8_2	4.10E+06	2.03E+09	5.55 ^f ± 0.07
GR0082_8_3	4.18E+06	2.07E+09	5.99 ^f ± 0.07
GR0081_19_1	4.17E+06	2.07E+09	6.59 ^c ± 0.09
GR0081_19_2	4.05E+06	2.01E+09	5.29 ^f ± 1.14
GR0081_19_3	4.07E+06	2.02E+09	6.53 ^f ± 0.06
GR0081_6_1	4.10E+06	2.04E+09	5.57 ^f ± 0.05
GR0081_6_2	4.18E+06	2.07E+09	5.99 ^f ± 0.05
GR0081_6_3	4.05E+06	2.01E+09	5.41 ^f ± 0.07
GR0081_23_1	4.18E+06	2.07E+09	6.39 ^f ± 0.06
GR0081_23_2	4.23E+06	2.10E+09	6.40 ^f ± 0.07
GR0081_23_3	4.17E+06	2.07E+09	6.55 ^f ± 0.08
<i>Mount GRIN_2</i>			
GR97m27_14_1	4.24E+06	2.08E+09	13.50 ^c ± 0.06
GR97m27_14_2	4.11E+06	2.03E+09	11.20 ^c ± 0.11
GR97m27_23_1	4.25E+06	2.09E+09	14.20 ^f ± 0.07
GR97m27_23_2	4.25E+06	2.10E+09	14.30 ^f ± 0.06
GR97m27_29_1	4.15E+06	2.04E+09	14.10 ^c ± 0.06
GR97m27_29_2	4.25E+06	2.10E+09	14.40 ^c ± 0.05
GR97m27_31_1	4.28E+06	2.10E+09	14.50 ^c ± 0.09
GR97m27_31_2	4.20E+06	2.08E+09	14.70 ^c ± 0.06
GR97m27_24_1	4.21E+06	2.07E+09	16.60 ^c ± 0.07
GR97m27_35_1	4.33E+06	2.13E+09	13.90 ^f ± 0.08
GR97m27_35_2	4.31E+06	2.12E+09	13.70 ^f ± 0.07
GR97m27_38_1	4.19E+06	2.05E+09	13.30 ^f ± 0.07
GR97m27_38_2	4.12E+06	2.04E+09	13.10 ^f ± 0.05

^a Oxygen isotope values are expressed in per mil deviations from standard mean ocean water (SMOW). Errors reported as 1σ internal error. IMF determined by difference of known $\delta^{18}\text{O}$ of AS3 and weighted mean and standard deviation of AS3 analyses from the same mount as unknowns; GRIN_1 IMF = -1.04 ± 1.80 , GRIN_2 IMF = $+0.60 \pm 0.99$ (1σ external errors).

suggests that reequilibration was limited to Pb isotopes and did not extend to whole scale disturbance of compatible trace elements such as U and Th.

GR04031 is a granodioritic orthogneiss from the same package of Ag units as GR04051 (Fig. 3C). Twenty-three analyses on 23 grains yield several poorly defined populations (Fig. 6B), the oldest of which is assigned a magmatic origin with a weighted mean age of 3693 ± 19 Ma (MSWD = 1.1, $n = 4$) and a tightly grouped population of igneous-like Th/U ratios (0.40 ± 0.06). Three younger zircon populations have much wider distributions in Th/U (Table 1) accompanied by variable internal zoning

(EA-5) and are interpreted to be from zircon growth or reequilibration during metamorphism.

GR04050 is a quartz monzodioritic orthogneiss, located just west of and running parallel to, GR04031 and GR04051. It is in a cross-cutting relationship with an amphibolite unit directly to the west. The oldest zircon population has a weighted mean of 3648 ± 42 Ma (MSWD = 9.0, $n = 5$) with Th/U ratios of 0.41 ± 0.18 . The next oldest zircon population (3534^{+27}_{-29} Ma, $n = 3$) has a similar Th/U ratio (0.38 ± 0.21) and cannot be eliminated as potentially magmatic on that basis (Fig. 6C). However, because of the low zircon saturation temperature (740°C , EA-1), it seems unlikely that an older population would have persisted for any significant length of time during melt emplacement, and therefore we view the older population (~ 3650 Ma) to represent the minimum age of emplacement for this unit.

GR04035 is a granodioritic orthogneiss found in a small exposure to the north of, and along strike with GR04031, GR04050 and GR04051. Twenty-one analyses from 20 zircons yield a complicated age spectrum with three discernable age populations (Fig. 6D). The oldest population (3701 ± 15 Ma) is magmatic based on Th/U ratios (Table 1). The second oldest population (3649^{+22}_{-20} Ma) also has magmatic-like Th/U (Table 1), but the older age is favored because of the low zircon saturation temperature (662°C , EA-1). The third zircon population is metamorphic at 3553 ± 27 Ma with Th/U = 0.09 ± 0.13 and dark, unadorned cores in CL.

GR04032 is a dioritic orthogneiss from the south-easternmost exposure of Ag that appears to intrude a quartz–biotite schist (Aqb). Fourteen spots from 12 grains were analyzed. The oldest age was obtained from a concordant 3677 ± 13 Ma zircon (grain 07_1 EA-2; Fig. 6E), but we note that there is only one analysis of this age and it has elevated $[\text{Th}/\text{U}]_{\text{Zr}}$ (1.06). Despite the low saturation temperature (698°C , EA-1), this grain may be inherited. A more likely crystallization age is 3553 ± 10 Ma (weighted mean), represented by three analyses with similar Th/U ratios ($\sim 0.52 \pm 0.04$) that we interpret to be consistent with a magmatic *in situ* origin and corresponds to a metamorphic age recorded in adjacent orthogneisses.

GR04033 is a tonalitic orthogneiss adjacent to GR04032. Five (discordant) zircons measured from this sample were younger than 3550 Ma (EA-2). This rock is interpreted to be similar in age to GR04032 and may in fact be part of the same unit, perhaps as a selvage.

4.1.2. Candidate rock for sedimentary protolith—east outcrops

Sample GR04034 is a magnetite-bearing, quartz–plagioclase–biotite schist (Aqb) located directly east of samples GR04032 and GR04033 (Fig. 2). Zircons from this unit are 50–400 μm in length with the larger zircons irregularly shaped and the smallest uniformly round (EA-5). Eleven spots from 11 grains were analyzed (Fig. 6F). There are two old populations at (weighted means) 3614 ± 13 Ma

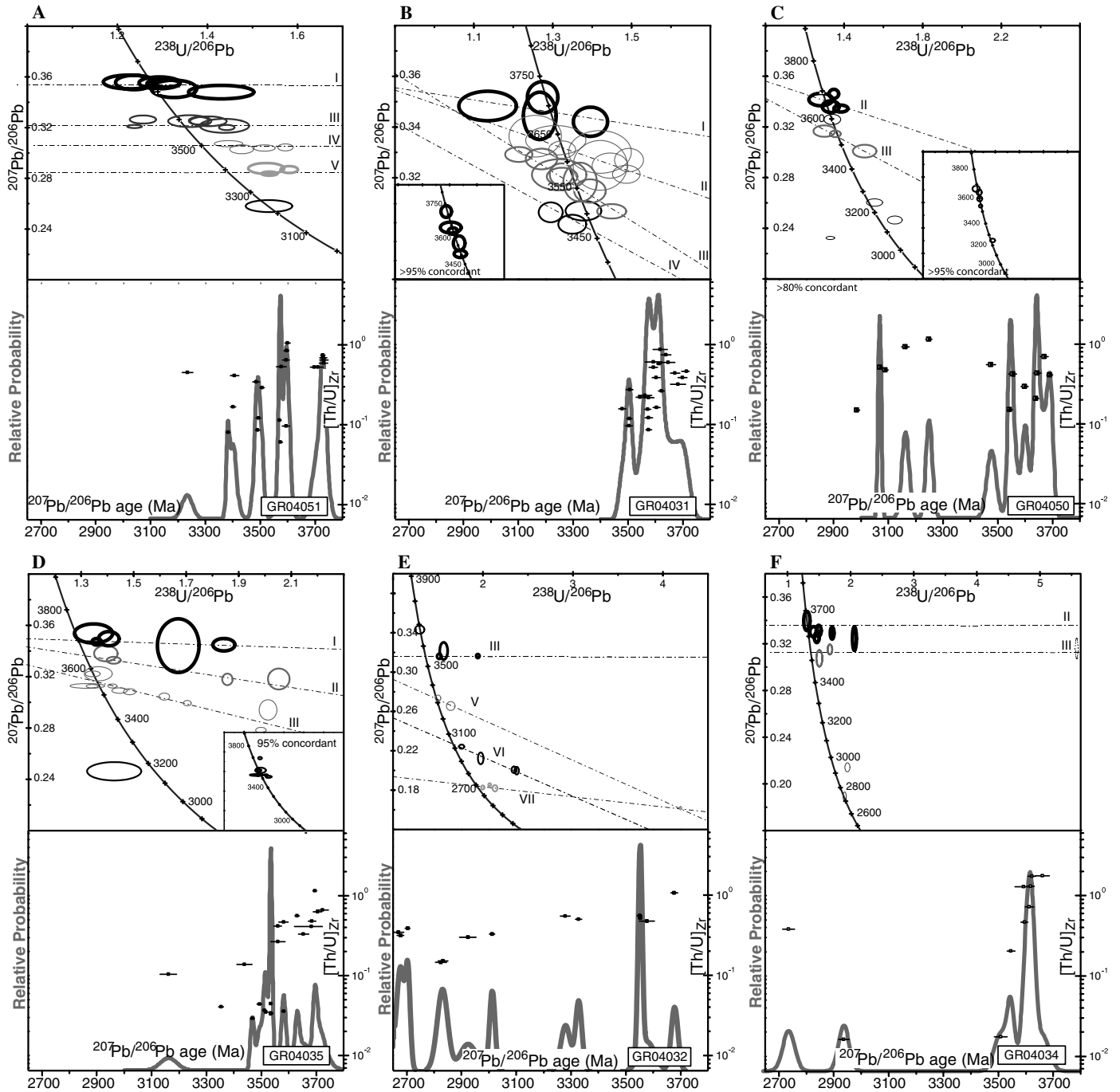


Fig. 6. Integrated geochronology and Th/U geochemistry of zircons from samples on the eastern side of island west of Innersuartuut (Fig. 2). Upper panels are Terra-Wasserberg plots with populations corresponding to separate events (1σ error ellipses, see EA-2; Ludwig, 2001). Lower panels are integrated probability and Th/U_{zircon} (1σ error bars; EA-2). (A) GR04051; (B) GR04031; (C) GR04050; (D) GR04035; (E) GR04032; (F) GR04034.

(MSWD = 1.3, $n = 6$) and 3536 ± 24 Ma (MSWD = 1.8, $n = 2$), both with a wide range of Th/U ratios (0.02–1.7). We interpret all sampled zircons in this unit are the result of *in situ* metamorphic growth.

4.1.3. Western Ag units

Sample GR04036 is a biotite-rich, mafic gneiss from the southwest quadrant of Case Study 1 (Fig. 2). The unit is narrow (<50 cm) and completely dissects a quartz–garnet

rock *Agg* (GR04037; Fig. 3C). Twenty analyses on 20 zircons show that most grains have experienced significant Pb-loss (13/20 are >50% discordant; Fig. 7A, inset). Pb-loss expressed by discordance seems to have a recent component (Fig. 7A, inset); data were filtered to include only grains with >50% concordance. The two oldest analyses (grains 20 and 11; EA-2) are within 15% of concordia at 3755 ± 12 Ma (86% concordant) and 3695 ± 17 Ma (92% concordant) with igneous-like Th/U ratios (0.38 and 0.58,

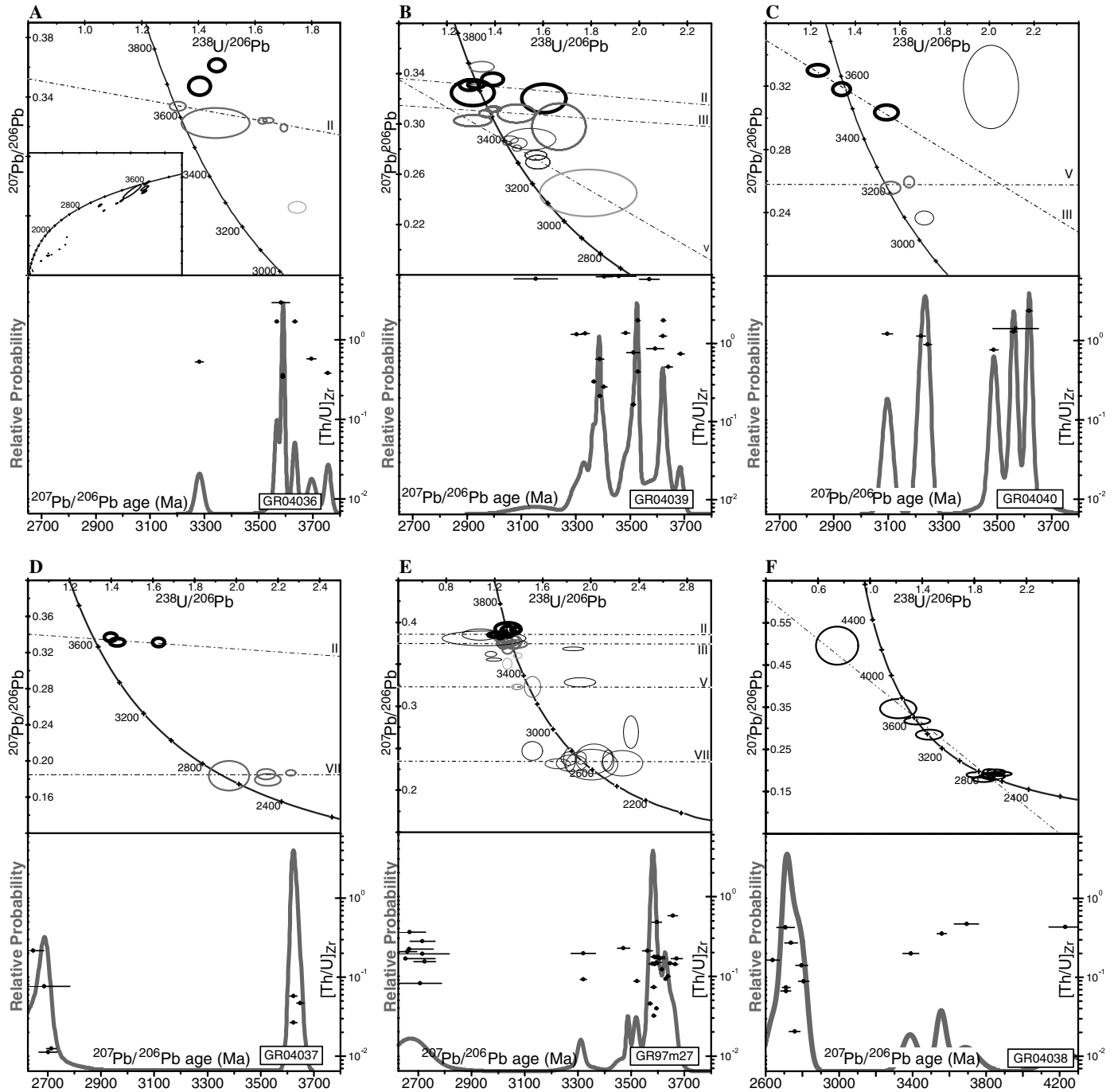


Fig. 7. Integrated geochronology and Th/U geochemistry of zircons from samples on the western side of island west of Innersuartuut (Fig. 2). Upper panels are Terra-Wasserberg plots with populations corresponding to separate events (1σ error ellipses, see EA-2; Ludwig, 2001). Lower panels are integrated probability and Th/U_{zircon} (1σ error bars; EA-2). (A) GR04036; (B) GR04039; (C) GR04040; (D) GR04037; (E) GR97m27; (F) GR04038.

respectively) and cores with oscillatory zoning in CL. When combined, they yield a weighted age of 3735 ± 360 Ma (MSWD = 8.5). The only clear population is 3637^{+23}_{-19} Ma (Table 1) with a wide range of Th/U (1.4 ± 1.1) and mostly disrupted or absent zoning in CL (EA-5). A final 86% concordant analysis yields an age of 3282 ± 15 Ma. From these data, the most likely magmatic (emplacement) age is ~ 3750 Ma, providing a lower limit to the age of the *Aqg* unit that it intrudes. Our interpretation

of these data is that the rock was affected by metamorphic events starting at 3637^{+23}_{-19} Ma.

Sample GR04039 is an augen gneiss from a package of *Ag* units that appears to penetrate the quartz–garnet schist (*Aqg*) and may also cross-cut the *Am–Aqg* contact, although the contact is obscured by a pegmatite (EA-1). Twenty analyses from 19 grains yield a complicated age spectrum (Fig. 7B). One zircon (grain 27) yielded a 96% concordant age of 3687 ± 12 Ma (Th/U = 0.74). The

oldest age population is 3623 ± 12 Ma (Table 1). There are also two other populations at 3519 ± 10 and 3405^{+87}_{-22} Ma. All populations have highly variable Th/U (Table 1), suggesting that chemical and isotopic disturbance was probably widespread and recorded ages are metamorphic.

Sample GR04040 is a mafic gneiss located within a meter of GR04039 (EA-1). The age distribution is bimodal (Fig. 7C), with the older population yielding an upper intercept of 3562^{+28}_{-27} (MSWD = 0.41, $n = 3$, Th/U = 1.4 ± 0.8), and a younger population with a poorly defined weighted mean age of 3200 ± 180 Ma (MSWD = 19, $n = 3$; Th/U = 1.1 ± 0.17). A final, highly discordant grain with a $^{207}\text{Pb}/^{206}\text{Pb}$ age of 3568 ± 84 Ma was not included in our calculations. Because only seven zircons were analyzed and the Th/U ratios are so variable and high and zircons are only weakly zoned in CL (EA-5), an upper age of ~ 3560 Ma is tentatively assigned as metamorphic and therefore merely defines the minimum age of the rock.

4.1.4. Candidate rocks for sedimentary protolith—west outcrops

Sample GR04037 is a quartz–garnet rock (Aqq) with abundant biotite which is bisected by GR04036 (3755 ± 12 Ma). Zircons from this unit are small ($<100 \mu\text{m}$) and rare. They are irregularly shaped and typically rounded, some appear to be broken crystals. They have a simple age spectrum (Fig. 7D), with two age groups: a dominant one at 3632 ± 16 Ma, and another at 2702 ± 30 Ma and very low Th/U ratios (0.08 ± 0.09 and 0.04 ± 0.015) indicating that both are metamorphic, having grown *in situ* during known events that affected West Greenland in the Archean (Table 1).

Sample GR97m27 is a quartz–garnet rock with both amphibole and biotite that makes up a significant portion of the northwest portion of the island (Fig. 3A). This rock is in contact with the Ag package that includes GR04039 and GR04040 (EA-1). Zircons from this unit were small ($30\text{--}110 \mu\text{m}$) and round and the size distribution is bimodal (EA-5). Forty zircons were analyzed from a 2 kg sample separate and the data filtered to exclude analyses greater than 15% discordant and less than 98% $^{206}\text{Pb}^*$ (Fig. 7E) and fall into four age categories (reported ages are weighted means; Table 1): (i) the youngest and most clearly defined is at 2690 ± 38 Ma (Th/U = 0.21 ± 0.08); (ii) two analyses fall at 3320 ± 22 Ma (Th/U = 0.14 ± 0.07); (iii) the third group is 3590 ± 8 Ma (Th/U = 0.77 ± 0.03); and (iv) the oldest group falls at 3643 ± 17 Ma (U/Th = 0.15 ± 0.11). The break between the oldest two groups is not clear and may in fact be the same group that had experienced early Pb-loss, and when combined they yield an age of 3609 ± 14 (MSWD = 8.9). However, the high MSWD suggests that there is more than one population present. The older age is contemporaneous with the onset of granulite facies metamorphism (Griffin et al., 1980) and the younger ages could reflect *in situ* solid-state re-equilibration/recrystallization (e.g., Hoskin and Black,

2000) at ca. 2700 Ma (Table 1) an event previously recorded by zircon geochronology in the *Færinghavn terrane* (e.g., Nutman et al., 1996).

Sample GR04038 is an Aqq rock, likely part of the same unit as GR97m27 on the northernmost part of the west side of the island (EA-1). Zircon morphologies are similar between the two rocks. All zircons from GR04038 fall along a single discord with intercepts at 3642 ± 160 and 2707 ± 130 Ma (MSWD = 1.7), with the majority (8/12) of analyses at ~ 2700 Ma (Fig. 7F). These relations provide an excellent recorder of metamorphism affecting the *Færinghavn terrane* since the Eoarchean. Th/U ratios for the youngest zircons are 0.16 ± 0.13 . Of the four remaining analyses, three are $<95\%$ concordant with ages of 3692 ± 67 , 3558 ± 27 , and 3390 ± 43 Ma, and one outlier (grain 15_1, EA-2) is reversely discordant at 4200 Ma (re-analysis of this grain yielded an age of ~ 3550 Ma).

4.2. Case Study 2: Qilangaarsuit

Sample GR04066 is a granodioritic biotite–garnet gneiss that dissects one of the ultramafic lobes (Fig. 4). It contains a large number of leucosomes, such that avoiding zircons from *in situ* melt patches is impossible. Zircons are relatively rare, mostly quite rounded and weakly zoned in CL with thin bright rims (EA-5). Twelve analyses on 11 grains yielded an isochron with an upper intercept of 3671^{+38}_{-35} Ma (MSWD = 0.86; Fig. 8A). Three analyses yield a slightly discordant young population with a weighted mean age of 2713 ± 30 Ma (Table 1). A discordia with a lower intercept anchored at 2713 ± 30 Ma produces an upper intercept of 3696^{+42}_{-40} Ma (MSWD = 0.78). The oldest single zircon analysis is 3657 ± 13 Ma coincident with the oldest metamorphic event common to this region (Table 1). Th/U ratios for the oldest analyses are typical for igneous precursors (0.45 ± 0.11 , $n = 3$), whereas more discordant zircons on the discord have a wider range of Th/U (0.36 ± 0.20 , $n = 6$), and youngest population has metamorphic Th/U ratios (0.05 ± 0.03 , $n = 3$). Our interpretation of these data is that crystallization of these zircons took place at 3696^{+42}_{-40} Ma, followed by minor open system behavior, probably during early metamorphism at granulite facies ca. 3650 Ma, with a second period of metamorphism at 2713 ± 30 Ma and minor recent Pb-loss that has affected most of the zircons.

GR04057 is a tonalitic gneiss infolded in an amphibolite unit at the northernmost extent of the ultramafic lobes near the limit of the outcrop (Fig. 4). Zircon morphologies are similar to GR04066 (EA-5). Eleven analyses on 11 grains yielded a discordia with an upper intercept of 3692 ± 90 Ma (MSWD = 4.4; Fig. 8B) when one highly discordant (37%) analysis is excluded. As with GR04066 there appear to be two age populations that are coincident with major metamorphic events in the *Færinghavn terrane* (Table 1): at 3668 ± 21 and at 2715 ± 13 Ma. Two additional analyses have a weighted mean age of 3596 ± 10 Ma, which may represent a

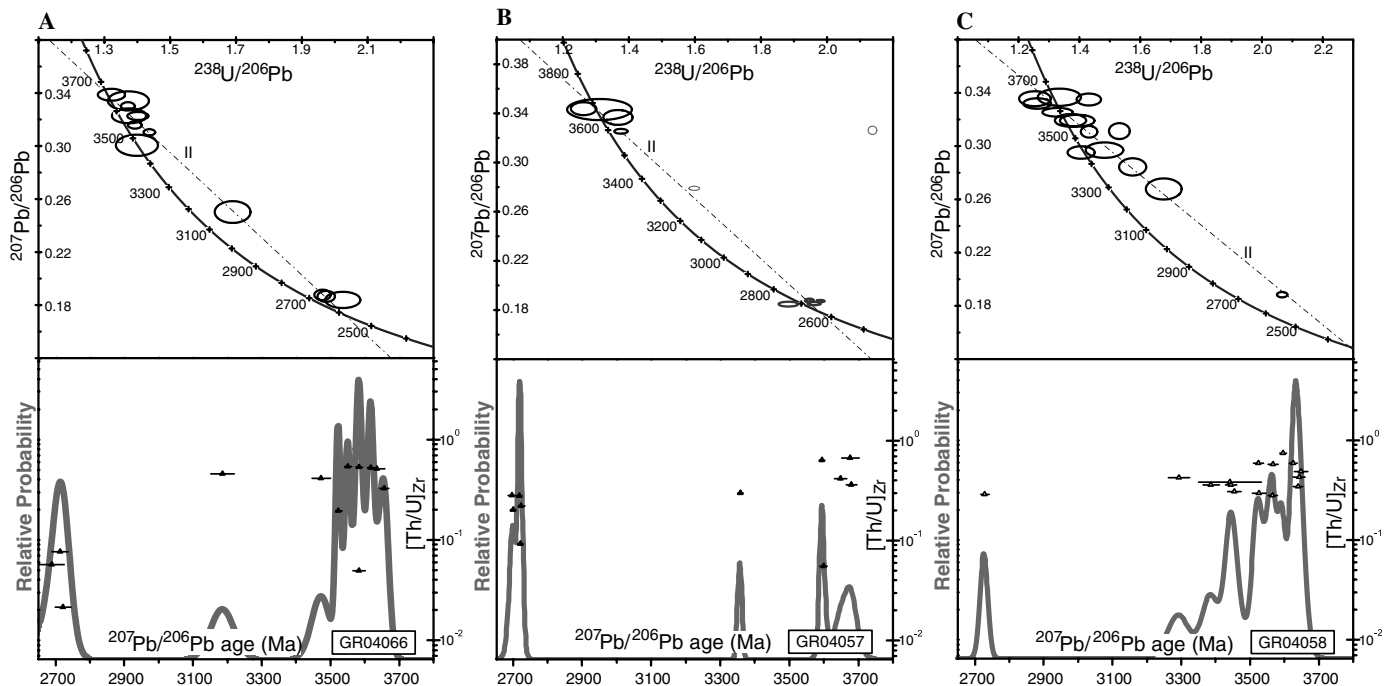


Fig. 8. Integrated geochronology and Th/U geochemistry of zircons from samples on Qilangaarsuit (Fig. 4). Upper panels are Terra-Wasserberg plots with populations corresponding to separate events (1σ error ellipses, EA-2). Lower panels are integrated probability and Th/U_{zircon} (1σ error bars; EA-2; Ludwig, 2001). (A) GR04066; (B) GR04057; (C) GR04058.

discrete metamorphic event ($\text{Th}/\text{U} = 0.35 \pm 0.41$) or grains of the older population with disturbed systems. The final analysis is slightly discordant at 3358 ± 6 Ma and possibly represents a mixture of domains during analysis. The older population has typical igneous Th/U ratios of 0.48 ± 0.17 , whereas the younger population has a value of 0.22 ± 0.07 .

4.2.1. Candidate rock for sedimentary protolith

GR04058 is a garnet–biotite–anthophyllite schist that occurs as thin, discontinuous lenses paralleling the foliation trend in the granitoid gneisses. Zircons are abundant, elongate with rounded tips and are typically larger than those of GR04066 and -57. Grains are strongly zoned in CL, often with cores showing interrupted zoning. Fifteen analyses from 15 zircons yield a discordia with an upper intercept of 3619 ± 67 Ma (Fig. 8C, Table 1) when a single highly discordant analysis is excluded. The oldest four analyses have a weighted mean of 3636 ± 14 Ma (Table 1). Other analyses do not group into a single age, but rather string along the discordia, and are therefore considered likely to represent isotopically disturbed older zircons with Th/U ratios of 0.43 ± 0.14 .

4.3. Case Study 3: Western innersuurtuut

Three TTG-type gneisses and a paragneiss (EA-1) from the mapped outcrop (Fig. 5) on the main island of Innersuurtuut were prepared for zircon U–Pb geochronology. Zircons from the orthogneisses are similar with high aspect ratios and most have cores with oscillatory zoning in

contrast to zircons from the paragneiss which are smaller, more rounded and poorly zoned (EA-5).

4.3.1. Orthogneiss units

Sample GR0081 is a relatively undeformed, granodioritic gneiss from a narrow (15–25 cm) sheet that penetrates an Aqp unit (GR0096) just to the north of the mapped outcrop. Ten points from 10 grains were analyzed and the oldest grain (25_1 EA-2) yields a 95% concordant age of 3594 ± 6 Ma and a magmatic-type Th/U ratio of 0.46 ± 0.01 , however, the oldest population in the sample is 3534 ± 10 Ma (Fig. 9A) and also has a Th/U ratio of 0.36 ± 0.09 , consistent with a magmatic origin (Table 1). Younger populations have lower and more variable Th/U ratios consistent with metamorphic growth. We interpret the 3594 ± 6 Ma age as the time of emplacement, but we cannot rule out the 3535 ± 9 Ma age as magmatic based solely on Th/U ratios. In light of the fact that this unit is relatively undeformed and preserves outstanding cross-cutting relationships, a younger magmatic age would be consistent with the field observations.

Sample GR0082 is a trondhjemitic gneiss that penetrates the Aqp rock. Ten analyses on 10 grains yielded two populations (Fig. 9B), the oldest of which at 3629 ± 7 Ma (Table 1) is interpreted to be magmatic. The younger population is 3586 ± 8 Ma. If pooled, the populations yield a non-statistically significant discord with an age of 3630 ± 30 Ma with a MSWD of 17. The Th/U ratios of the two populations are both consistent with a magmatic origin (0.53 ± 0.10 and 0.41 ± 0.17 ,

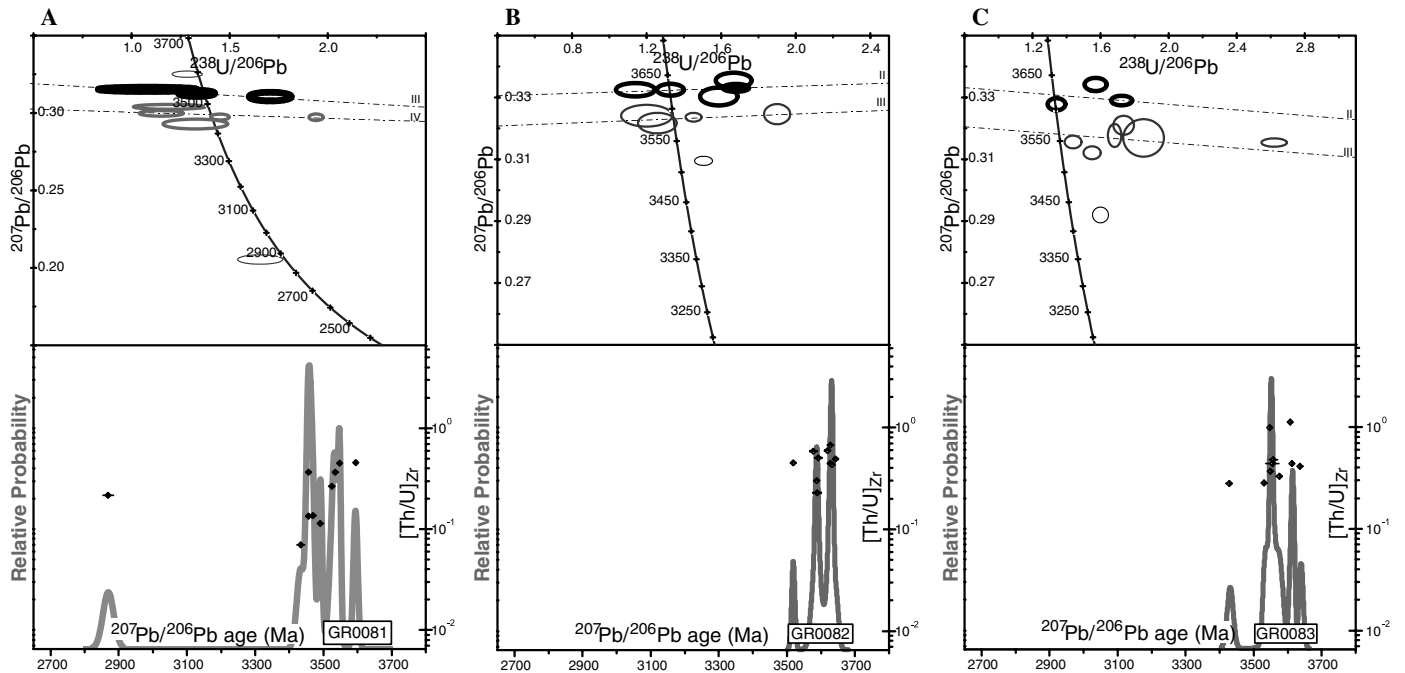


Fig. 9. Integrated geochronology and Th/U geochemistry of zircons from samples on Innersuaqtuut (Fig. 5). Upper panels are Terra-Wasserberg plots with populations corresponding to separate events (1σ error ellipses, see EA-2). Lower panels are integrated probability and Th/U_{zircon} (1σ error bars; EA-2; Ludwig, 2001). (A) GR04081; (B) GR04082; (C) GR04083.

respectively) and the age of emplacement cannot be determined on that basis (Table 1). However, the zircon saturation temperature of 774 °C for the rock suggests that the older age is more likely as zircons are unlikely to persist in a strongly zircon undersaturated magma.

Sample GR0083 is a tonalitic gneiss. Ten analyses on 10 grains yield potentially two populations statistically identical to those of GR0082 (Fig. 9C). Most grains appear to have been affected somewhat by recent Pb-loss and ages are reported as weighted means. The oldest population is 3617 ± 34 Ma ($n=3$, MSWD = 6.1) and the younger population is 3548 ± 13 Ma ($n=6$, MSWD = 2.6). If pooled these data yield a non-statistically significant discordia of 3684 ± 290 Ma (MSWD = 30) or a weighted mean of 3579 ± 29 Ma (MSWD = 35). As with GR0082 these populations are not distinguishable on the basis of Th/U (Table 1), but the older age is favored based on the low zircon saturation temperature (779 °C) for this rock.

4.3.2. Candidate rock for sedimentary protolith

Sample GR0096 is a pyroxene-bearing, quartz–biotite–garnet schist with variable grain size. Only one zircon (grain 28_1) was analyzed by standard U–Pb ion microprobe methods and yielded an 18% discordant grain with an age of 3595 ± 6 Ma and a Th/U ratio of 1.02 ± 0.01 . Preliminary $^{207}\text{Pb}/^{206}\text{Pb}$ ages obtained by multicollector mode Turner et al. (2004) on 28 grains yielded an age spectrum in which no analyses were greater than 3609 ± 10 Ma and we interpret all grains to be of metamorphic origin.

5. Zircon oxygen isotope compositions

Primary zircon oxygen isotopic values can be preserved at even the highest metamorphic grades, particularly under anhydrous conditions (Valley et al., 1994; Watson and Cherniak, 1997; Valley, 2003). These data can be used to provide a firm measure of $\delta^{18}\text{O}_{\text{Zr}}$ at the time of formation over (multi-mineralic) whole-rock analyses, which may be subsequently re-equilibrated in oxygen due to invasive fluids (Valley et al., 2003). To test this hypothesis, we have measured the oxygen isotopic composition of zircons from selected samples that had previously been used for U–Pb geochronology and correlate our $\delta^{18}\text{O}_{\text{Zr}}$ results with whole rock ($\delta^{18}\text{O}_{\text{WR}}$) and mineral (quartz, magnetite) values. Spot analyses were made after careful polishing of the grains to remove all traces of older sputter pits from past analytical sessions. Furthermore, care was taken to position oxygen analysis spots adjacent to zones in the individual crystals where reliable ages have been obtained and away from cracks (EA-5).

5.1. TTG-composition gneisses from Case Study #3

Samples GR0081–83 are tonalitic to granodioritic and range in age from ca. 3550–3630 Ma. Whole-rock oxygen isotope composition ($\delta^{18}\text{O}_{\text{WR}}$ vs. SMOW) for granodioritic gneiss sample GR0081 is +9.2‰ and the average $\delta^{18}\text{O}_{\text{Zr}}$ value is +6.1‰ (± 0.8 , 1σ ; Table 4), which is well within the range of oxygen values for rocks of this type. Sample GR0082 is a trondhjemitic gneiss with $\delta^{18}\text{O}_{\text{WR}} = +8.1\text{‰}$ and average $\delta^{18}\text{O}_{\text{Zr}}$ composition of +6.2‰ (± 0.5 , 1σ ; Table

Table 4
Summary of whole-rock and mineral oxygen isotopic data

Sample	$\delta^{18}\text{O}_{\text{Zr}}^{\text{a}}$		$\delta^{18}\text{O}_{\text{WR}}$ Calculated ^b		$\delta^{18}\text{O}_{\text{WR}}$ Measured ^c		$\delta^{18}\text{O}_{\text{Qtz}}$ Measured ^c		$\delta^{18}\text{O}_{\text{Mag}}$ Measured ^c	
		1 σ		1 σ		1 σ		1 σ		1 σ
GR0081	+6.1	± 0.8	+8.3	± 0.8	+9.2	± 0.1				
GR0082	+6.2	± 1.6	+8.4	± 1.6	+8.1	± 0.1				
GR0083	+8.3	± 0.5	+10.5	± 0.5	+7.4	± 0.1				
GR0096					+6.8	± 0.1	+9.1	± 0.1	+0.6	± 0.1
GR97m27	+14.0	± 0.9	+16.2	± 0.9	+16.0	± 0.1	+16.4	± 0.1	+0.185	± 0.1

^a Mean, calculated from Table 3. 1 σ external errors.

^b Calculated whole-rock value based on $\delta^{18}\text{O}_{\text{Zr}}$ and rock-zircon fractionation of about +2.2 (Valley et al., 1994).

^c Measured whole-rock values by Laboratoire Oxygène.

4); one very rounded pink zircon (grain 12_1) has an age of 3619 ± 9 Ma and $\delta^{18}\text{O}_{\text{Zr}} = +8.6\%$ in stark contrast to the other measured grains (8_1 and 10_1, Table 3). It is interesting to note that grain 12_1 is more characteristic of a metamorphic zircon in morphology (extreme rounded habit), oxygen isotopes (elevated in ^{18}O) and $^{207}\text{Pb}/^{206}\text{Pb}$ discordance (EA-2). However, from the standpoint of U–Th composition and age GR0082_12_1 resembles other igneous grains. The homogeneity in oxygen composition of grain 12 coupled with it being 16% discordant could mean that this grain effectively equilibrated its oxygen with invasive fluids during the metamorphic event(s) responsible for Pb loss.

Tonalitic gneiss sample GR0083 is about the same age (3617 ± 34 Ma) and similar in gross composition to GR0082. Zircons measured for oxygen isotopic compositions (grains 12_1 and 33_1; EA-2) were >95% concordant. Grain 12_1 contains a resolvable “core” region in CL imagery that has $\delta^{18}\text{O}_{\text{Zr}} = +6.9\%$ and large oscillatory “overgrowths” with $\delta^{18}\text{O}_{\text{Zr}}$ values of +8.3 to +8.5‰ (Table 4). The ^{18}O -enriched regions enclosing the zircon core in grain 12_1 are likely the result of equilibration of growing (metamorphic) zircon with fluids; grain 33_1 from this same sample is 3607 ± 6 Ma, 99% concordant, has a metamorphic Th/U value of 1.13, rounded habit and $\delta^{18}\text{O}_{\text{Zr}} = +8.8\%$. The whole-rock $\delta^{18}\text{O}$ value of GR0083 is +7.4‰ (Table 4).

5.2. GR97m27 (Aqg) unit from Case Study #1

In addition to characterization of zircon, both whole-rock and mineral separate oxygen isotope measurements were performed on sample GR97m27 for which mineralogy and geochemical composition pointed to a probable sedimentary source. The $\delta^{18}\text{O}_{\text{WR}}$ value for this rock is +16.0‰; magnetite and quartz $\delta^{18}\text{O}$ values are +0.185‰ and +16.4‰, respectively (Table 4). Oxygen isotope quartz–magnetite thermometry (Bottinga and Javoy, 1975) indicates a Qtz–Mag equilibration temperature of 585 °C, consistent with reequilibration at amphibolite facies metamorphism. The average $\delta^{18}\text{O}_{\text{Zr}}$ for this unit (Table 4) predicts a whole-rock value of about +16.2‰ assuming a zircon–rock oxygen isotope fractionation of approximately +2.2‰ (Valley et al., 1994). Based on these results, as well as compositional studies linked to the geochronology (Section 4.1.4), zircons in this unit grew during at least

two metamorphic events at ca. 3650 and 2700 Ma (Table 1) and are indistinguishable from each other in oxygen isotope composition. These $\delta^{18}\text{O}_{\text{Zr}}$ values are among the highest reported for individual zircons (see Cavosie et al., 2005 for a recent compendium). Mojzsis et al. (2001) reported an overgrowth on a detrital Jack Hills zircon with values as high as $\delta^{18}\text{O}_{\text{Zr}} = +15.0 \pm 0.4\%$ and such values are probably representative of zircon growth in media dominated by ^{18}O -enriched (sedimentary) sources. Metamorphism of quartzitic paragneisses can lead to neof orm zircon growth with the breakdown of Zr-containing minerals such as biotite, garnet, amphibole, as well as dissolution–reprecipitation of trace zircon (if present) in e.g., an Ostwald-ripening process (Ayers et al., 2003). Taken together, zircon geochronology and whole rock, Qtz–Mag and zircon oxygen isotope geochemistry show that this rock is of sedimentary origin and was present during the earliest recorded regional metamorphic event to affect the *Itsaq Gneiss Complex* at ca. 3650 Ma. Our results are completely consistent with the minimum age estimate of ca. 3750 Ma for this unit based on cross-cutting relationships with orthogneisses.

6. Multiple sulfur isotope analyses

Mass-independently fractionated (MIF) sulfur isotopes are reported as permil deviations from the mass fractionation line defined by $\Delta^{33}\text{S} = 0\%$ (where $\Delta^{33}\text{S} (\%) = 1000[(1 + \delta^{33}\text{S}/1000) - (1 + \delta^{34}\text{S}/1000)^2]$; the term λ expresses the mass dependent fractionation relationship between $\delta^{33}\text{S}$ and $\delta^{34}\text{S}$; Papineau et al., 2005 and references therein). MIF sulfur isotopes on Earth are the product of gas-phase reactions on sulfur (H_2S , SO_2) in anoxic atmospheres (reviewed in Pavlov and Kasting, 2002). Enhanced solar ultraviolet radiation deep in the anoxic atmosphere led to the establishment of MIF sulfur isotopes in the Archean geological record. MIF S in marine sedimentary rocks indicates the effective absence of atmospheric O_2 and an ozone screen at time of sedimentation (Farquhar et al., 2000). It has been now widely documented that Archean sedimentary sulfides and sulfates can preserve resolvable mass-independent $|\Delta^{33}\text{S}| \geq 0.30\%$ values, which stands in contrast with almost all sulfides and sulfates younger than 2.32 Ga with mass-dependent $\Delta^{33}\text{S}$ values in the range -0.30 to $+0.30\%$ (Farquhar and Wing, 2003;

Mojzsis et al., 2003b; Bekker et al., 2004; Papineau et al., 2005). When combined with other supporting mineralogical and geochemical indicators, the presence of non-zero $\Delta^{33}\text{S}$ in an Eoarchean rock would be thoroughly consistent with its origin as sediment.

6.1. GR04063 banded iron-formation from Innersuartuut

A finely laminated quartz + magnetite \pm garnet banded iron-formation (EA-1) from the main island (N63°50.227', W51°41.173') was sampled for sulfur isotope analysis. This rock was collected approximately 500 m east of Case Study #3 because it preserves quartz–magnetite bands and apparently escaped the pervasive strain/recrystallization/silica-mobility recorded by *Aqp* units elsewhere. In this respect, it most resembles samples 119233 from Ugpik and 119217 from Innersuartuut described in McGregor and Mason (1977). Multiple sulfur isotope geochemistry of this rock, which experienced the same regional metamorphisms as all other samples described herein, provides a useful benchmark for the preservation of MIF S in the (granulite) *Færinghavn terrane*. Sulfides in this sample are present as pyrrhotite blebs in the quartz–magnetite matrix with fine intergrowths of SiO_2 (electronic annex EA-6). Pyrrhotites preserve consistently large $\Delta^{33}\text{S}$ values between $+1.31 \pm 0.19\text{‰}$ and $+1.49 \pm 0.19\text{‰}$ (2σ external errors) and record a small range in $\delta^{34}\text{S}$ of $\sim 1.5\text{‰}$ (Table 2).

6.2. GR04041, GR04054 and GR0096 quartz–pyroxene units (*Aqp*)

Ferruginous quartz–pyroxene rocks from Case Study #1 resemble both in mineralogy and gross geochemical composition samples G91-26 of Mojzsis et al. (1996; see Manning et al. 2006) and GR9707 of Mojzsis et al. (2003b) and contain abundant pyrrhotite and occasional chalcopyrite with subhedral habit in a dominantly quartz + hedenbergite matrix (EA-6). All analyzed pyrrhotites in these samples preserve MIF S isotopes (Table 2) with large $\Delta^{33}\text{S}$ values between $+1.90 \pm 0.25\text{‰}$ and $+3.15 \pm 0.25\text{‰}$ (2σ external errors) and range in $\delta^{34}\text{S}$ by $\sim 2.5\text{‰}$. Although recording a smaller total range in $\delta^{34}\text{S}$ compared to *Aqp* sample GR9707 ($\sim 12\text{‰}$) from Akilia (Mojzsis et al., 2003b), these samples preserve exceptionally large $\Delta^{33}\text{S}$ values akin to those reported for *ISB* banded iron-formation sample 248474 (Baublys et al., 2004; ca. $+3.3\text{‰}$) and repeated by Whitehouse et al. (2005). Sample GR0096 is a quartz–pyroxene unit on western Innersuartuut from Case Study #3 that contained rare blebs of small ($<100\ \mu\text{m}$) pyrrhotites grains in quartz with no resolvable MIF sulfur isotopes (Table 2; EA-6).

6.3. GR97m27 quartz–garnet–biotite schist unit (*Aqg*) from Case Study #1

Pyrrhotite grains are abundant in this sample (~ 1 mode %) and in back-scattered electron imagery (EA-6)

frequently contain intergrowths of magnetite + quartz similar to the Akilia quartz–pyroxene rock (sample GR9707) documented in Mojzsis et al. (2003a,b). All pyrrhotites analyzed contain MIF S isotopes (Table 2) with well-resolved $\Delta^{33}\text{S}$ values between $+0.67 \pm 0.21\text{‰}$ and $+0.98 \pm 0.12\text{‰}$ (2σ external errors) and range in $\delta^{34}\text{S}$ by $\sim 3\text{‰}$.

These results for mass-independent sulfur isotopes in granulite grade metamorphic mineral assemblages verify the observation that $\Delta^{33}\text{S}$ values in a rock containing accessory sulfur minerals are robust. The simplest explanation for the small spread of $\delta^{34}\text{S}$ values in these data, which follow normal mass-dependent laws, is by reprecipitation of sulfides during metamorphic processes (e.g., re-crystallization from low-temperature FeS_2 , to high-temperature Fe_{1-x}S phase changes). Dilution by invasive fluids (H_2S , etc.) carrying exotic sulfur does not appear to be an important process in rocks that contain no more than ~ 1 mode percent sulfur (Ohmoto, 1986). We find that scatter in $\Delta^{33}\text{S}$ values is minimal for each these units, which suggests that no significant foreign component of sulfur was added to the system since formation as aqueous sediments in the early ocean.

7. Discussion

Eoarchean upper amphibolite- to granulite facies enclaves of the *Akilia association* in southern West Greenland consist of variably deformed units of ortho-, para-, augen gneisses and migmatites, biotite- and mafic- to ultramafic gneisses and with intermixed ferruginous quartz–pyroxene, garnet–biotite schists and other rocks. Polyphase deformations endemic to this terrane are an imprint of the dynamic regime of several episodes of metamorphism that included at least one occurrence of *in situ* partial melting. It is noteworthy that partial melts are apparently absent in the northern *Isukasia* sector of the *Itsaq Gneiss Complex* (Nutman et al., 1996, 2004), so either the *Itsaq Gneiss Complex* represents the cross-section of an autochthonous terrane preserving a granulite (lower crust) to amphibolite facies (mid-crust) transition, or it is a composite (allochthonous) entity (Friend and Nutman, 2005a,b).

Since the “plate tectonics” system in a strict sense may not have operated in the Archean because of the enhanced thermal regime and concomitant differences in the rheology of the lithosphere, only cautious comparisons with contemporary rigid plate tectonics are warranted. In our view, the *Færinghavn terrane* rocks can be understood in the context of typical orogenic processes associated with crustal thickening, high thermal gradients enhanced on the early Earth, and compression possibly in one or more subduction regimes (Komiya et al., 1999). Under metamorphic conditions associated with plate collisions, deformation accompanies recrystallization, which tends to severely blur chrono-structural relationships except in rare instances where individual episodes of deformation can be defined. Greenstone belt formation from oceanic crust

metamorphism—including the chance preservation of original structures such as pillow lava features at Isua (Maruyama et al., 1991; Komiya et al., 1999)—is either not recognized or has not been preserved in the *Akilia association*. Unfortunately, the term “Isua Greenstone Belt” as recently promoted by Myers (2001), Fedo et al. (2001) and others to describe the rocks of the *Isua supracrustal belt (ISB)* is misleading; there are no actual “greenstones” in the Eoarchean upper amphibolite (Rollinson, 2001) to granulite facies (Griffin et al., 1980) rocks of West Greenland. Instead, the *ISB* is dominated by massive to foliated black amphibolitized mafic and ultramafic $Pl \pm$ garnet rocks. Lastly, the ubiquity of late tectonic leucogranites and pegmatoids throughout the Ameralik area and to the southern limits of the complex represent some of the last members of a long line of overprints to the gneiss complex and the supracrustal enclaves contained therein; these were likely generated by incipient melting during metamorphism.

As metamorphic rocks derive from pre-existing units of igneous, sedimentary or metamorphic origin, the composition of the protolith governs the gross mineralogical, chemical and isotopic compositions of the metamorphic products. The geologic setting for the origin of the *Akilia association* supracrustal rocks can begin to be understood by first documenting bulk compositions and trace element makeup. We integrate these data with isotope characters such as oxygen and multiple sulfur isotopes with detailed zircon geochronology to enable protolith assignment and age determination of these complex rocks.

7.1. Protolith assignment to mafic (*Am*), ultramafic (*Aum*) rocks

Trace element composition of rocks formed by igneous processes in the same tectonic environment with similar mineral compositions (i.e., rock type) is controlled by the composition of the source and bulk partition coefficients of the elements. Previous work in the *ISB* has found that trace element mobility is of great concern (e.g., Rose et al., 1996; Polat and Kerrich, 2001). In terranes which have reached granulite facies, element mobility was likely more widespread than at Isua, affecting elements that are generally immobile at greenschist or amphibolite facies. If elements remain immune to any subsequent alteration by other processes then there should be a linear covariance in the concentrations of these elements providing a simple test for element immobility.

For the amphibolite samples, we compared concentrations of the nominally immobile elements Ti, Zr, REE, Y and Nb to elements where mobility may be expected (Fig. 10). Ti, and the middle to heavy REE (HREE) appear to have been relatively immobile in all samples, light REE (LREE), Zr, Nb, and Y have been slightly disturbed in some samples and Rb, Ba and Sr are strongly disturbed. Based on the unusual major chemistry ($K_2O > 3.0$ wt.%) of *Am* samples *GR04044* and *GR04049 (EA-1)* as well as

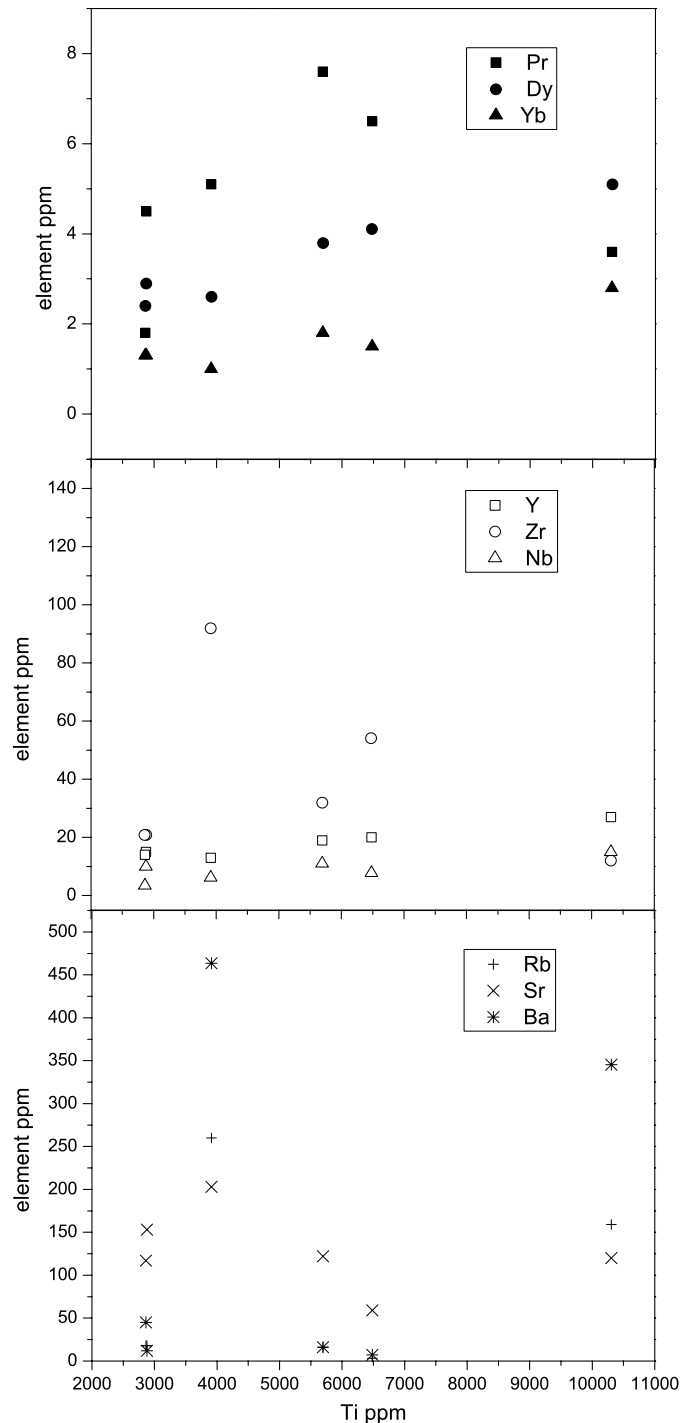


Fig. 10. Representative element vs. Ti concentrations of amphibolites (EA-1) showing differential mobility of elements, see text.

the apparent disturbance of some of the trace elements of these samples, they were excluded in tectonic discrimination. Bulk geochemistry of (mafic) amphibolite successions associated with candidate rocks for sedimentary protolith (e.g., *Aqq*)—*Am* samples *GR04044*, *-046*, *-048* and *-049* from Case Study #1 (island west of Innersuaartuut) and *Am* sample *GR04067* from Case Study #2 (Qilangaarsuit)—broadly agrees with a basaltic precursor. In major elements, the amphibolites are consistent with basalt com-

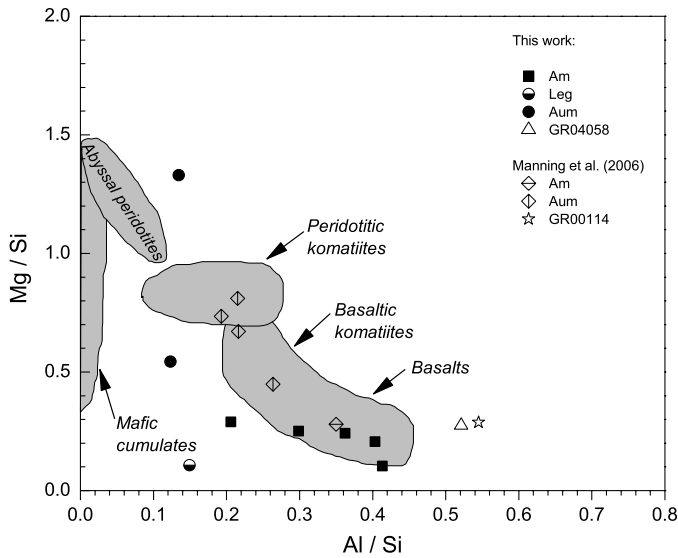


Fig. 11. Major element ratio plot (Al/Si vs. Mg/Si) of mafic/ultramafic rocks from the *Akilia association* and potential mafic detrital sediments (GR04058 and GR00114) superimposed on typical ratio fields for specific rock types.

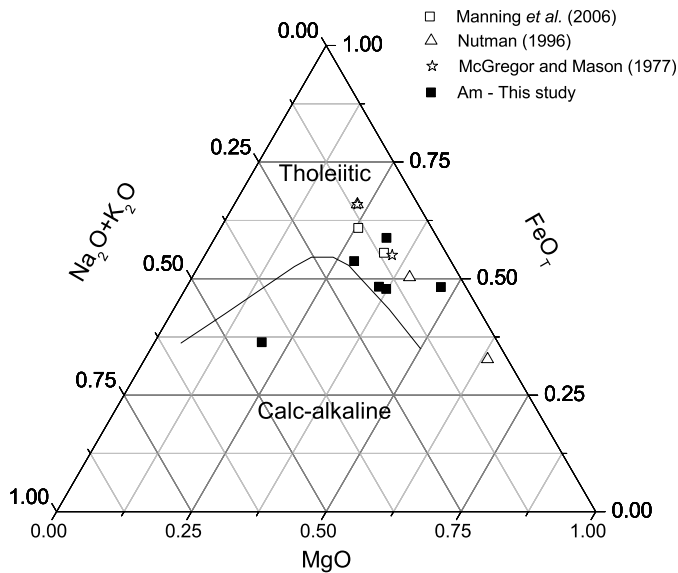


Fig. 12. AFM diagram (boundary of Irvine and Baragar, 1971) showing tholeiitic affinity of *Am*-type units in *Akilia association*.

positions on a plot of Mg/Si vs. Al/Si (Fig. 11) and consistent with tholeiites on an AFM plot (Fig. 12). Amphibolites are LREE enriched with variable to no Eu anomaly (Fig. 13), similar to some *Am* units reported from *Akilia* (Manning et al., 2006), but contrast with amphibolites from other *Akilia association* rocks (McGregor and Mason, 1977; McLennan et al., 1984; Nutman et al., 1996) and those at Isua (Frei et al., 2002; Polat et al., 2003) which are flat to very slightly LREE enriched. Because of the apparent disruption in the trace element geochemistry, particularly for large ion lithophile elements, tectonic discrimination based on expanded element patterns may be misleading (Fig. 14). However, key relationships of the

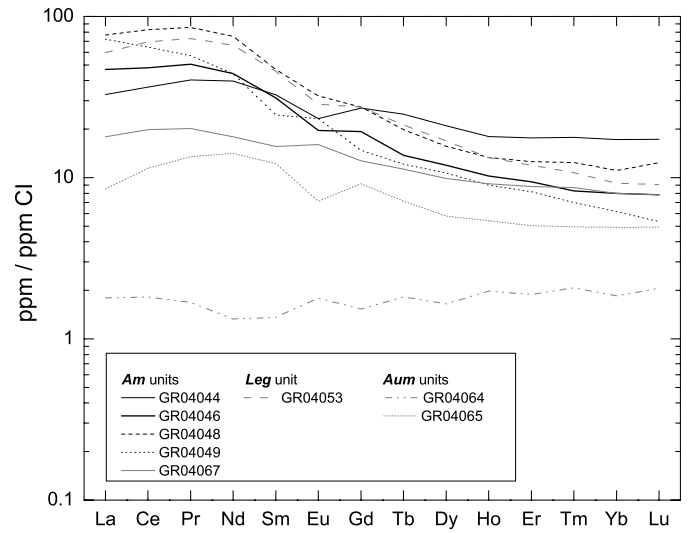


Fig. 13. REE diagram of mafic/ultramafic rocks from this study. Chondritic values from Anders and Grevesse (1989).

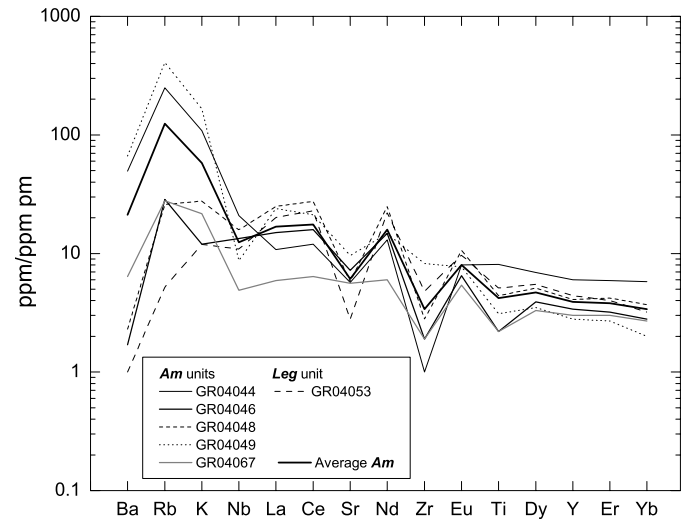


Fig. 14. Multi-element diagram of mafic rocks from this study. Primitive mantle values from McDonough et al. (1992).

least disrupted elements are likely to be informative. The amphibolites are characterized by small negative Nb anomalies, and negative Sr, Zr and Ti anomalies overlain on a generally negative to flat slope. Negative Nb anomalies are associated with the involvement of fluid-modified mantle wedge melting and are generally absent in oceanic plateaus. Data for the amphibolites plot near the fields of typical island-arc tholeiites in the ternary discrimination diagram of Pearce and Cann (1973; Fig. 15) as do other amphibolite units from the region. Isua amphibolites, though plotting within the island-arc field, appear to be enriched in Zr, and in fact many of the Isua samples plot within the continental arc field of Pearce (1983; Fig. 16). Because the quantity of *extrusive* mafic igneous rocks preserved in the crust volumetrically prevails over plutonic equivalents (Carmichael, 1989) we follow McGregor and Mason (1977) and interpret the *Am* units in geologic context with units *Aqp* and *Aqg* to have dominantly been lava

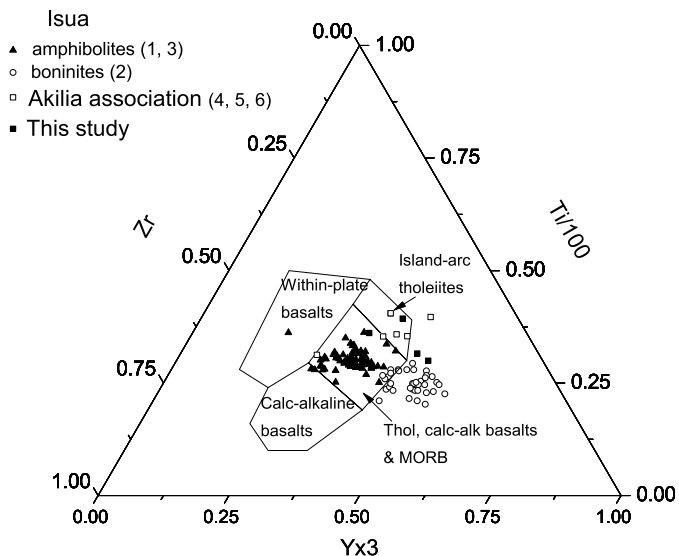


Fig. 15. Tectonic discrimination diagram of *ISB* (triangles and circles) and *Akilia association* (squares) mafic rocks. Fields of Pearce and Cann (1973). (1) Polat et al. (2003); (2) Polat et al. (2002); (3) Polat and Hofmann (2003); (4) Manning et al. (2006); (5) McGregor and Mason (1977); (6) Nutman et al. (1996).

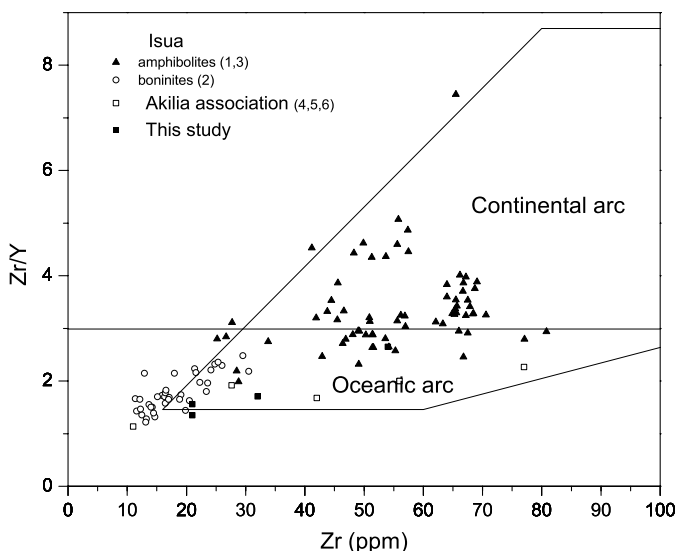


Fig. 16. Tectonic discrimination diagram of *ISB* (triangles and circles) and *Akilia association* (squares) mafic rocks showing oceanic arc affinity for *Akilia association* amphibolites. Fields of Pearce (1983). See Fig. 15 for references.

flows or some other volcanic rock intercalated with sea-floor sediments at time of formation. Given the compositions of these rocks, they formed in a plate margin and may have originated in a back-arc setting.

Compositionally, the ultramafic (*Aum*) samples *GR04064* and *-065* appear as intermediates between abyssal peridotite and basaltic komatiite, respectively (Figs. 11 and 13). Rocks with the composition of *GR04064* are usually mantle-derived and this particular sample strongly resembles ultramafic rocks ascribed a harzburgitic or abyssal peridotitic parentage in other *Akilia association* enclaves

(Friend et al., 2002b; Bennett et al., 2002). Sample *GR04065* may have been a gabbroic member of komatiite + basalt oceanic crust, and CaO + MgO contents are elevated relative to typical basalt compositions (EA-1).

7.2. Protolith assignments to candidate sedimentary units—ferruginous quartz–garnet mica (*Aqg*), quartz–pyroxene (*Aqp*) and aluminous quartz–biotite (*Aqb*) rocks

A plot of major element compositions for the siliceous garnet-quartz (*Aqg*; Section 2.2.1) and aluminous *Aqb* unit in Case Study #1 and *GR04058* (Case Study #2; Section 2.3.1) compared in Fig. 17A with a database of banded iron-formation lithologies from the *Isua supracrustal belt* (Dymek and Klein, 1988) and various supracrustal types described for the *Akilia association* (McGregor and Mason, 1977; McLennan et al., 1984; Fedo and Whitehouse, 2002a,b; Manning et al., 2006) reveals generally higher TiO_2/P_2O_5 contents than most *Isua* iron formation samples

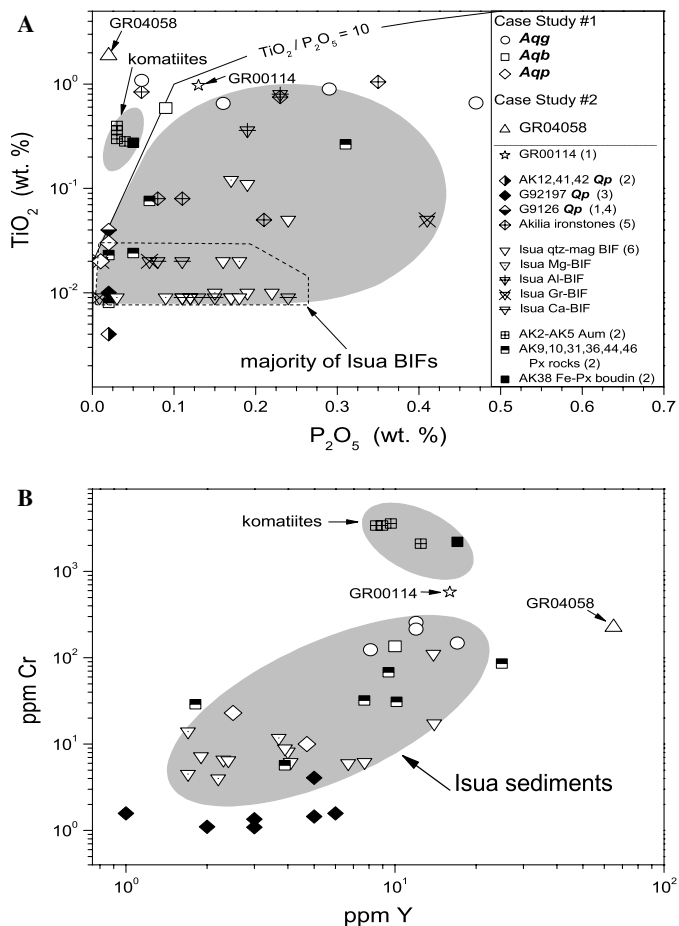


Fig. 17. (A) P_2O_5 vs. TiO_2 plot of *Akilia association* and *Isua supracrustal belt* (*ISB*) lithologies. (B) Y vs. Cr plot of *Akilia association* and *ISB* supracrustals. References: (1) Manning et al. (2006); (2) Fedo and Whitehouse (2002a,b); (3) Mojzsis et al., 1996; (4) Nutman et al. (1997); (5) McLennan et al., 1984; (6) Dymek and Klein (1988). Legend key: *Qp*, quartz–pyroxene rock; *qtz-mag BIF*, quartz–magnetite BIF; *Mg-BIF*, magnesian BIF; *Al-BIF*, aluminous BIF; *Gr-BIF*, graphitic BIF; *Ca-BIF*, carbonate BIF.

that have been reported in detail, but well within the field of sedimentary types. Sample *GR04058* (unit *Aqb*) from our Case Study #2 on Qilangaarsuit most resembles in overall chemistry a garnet–biotite schist noted by Manning et al. (2006) on Akilia (their sample *GR00114*). The close association of both garnet–biotite rocks to ultramafic assemblages in terms of field occurrence on Akilia and Qilangaarsuit is perhaps coincidental; the composition of these resembles that of pelagic clays derived from weathering of mafic lithologies. Neither unit is “in place”; they are infolded with surrounding lithologies, either granitoid gneisses in the case of *GR04058* or a mélange of mafic and ultramafic schists (*Au* in Manning et al., 2006) in the case of *GR00114*. The exclusively metamorphic zircons in both the Akilia and Qilangaarsuit *Aqb* sample appear to share a mutually indistinguishable formation date of 3636 ± 14 Ma (*GR04058*) and 3622 ± 30 Ma (*GR00114*; Manning et al., 2006); these ages are concurrent with the common assignment of the earliest high-grade metamorphic events in the *Føringhavn terrane*.

The quartz–pyroxene (*Aqp*) units (McGregor and Mason, 1977; McLennan et al., 1984) consistently plot (Fig. 17A and B) within the BIF field from Isua (Dymek and Klein, 1988) and both the *Aqp* units in our study and those on Akilia are demonstrably of sedimentary origin (Manning et al., 2006). The succession: ultramafic (komatiitic) flows (*Aum*)—basaltic flows (*Am*)—chemical sedimentary precipitate (*Aqp*) is typical for Eoarchean volcano-sedimentary series (Lowe and Byerly, 1999). If this interpretation is correct, a common lithologic association repeated on Akilia and widespread on Innersuartaq records a primary sequence with a likely minimum age of 3755 ± 11 Ma as defined by a narrow, 5-m long (granodioritic) mafic gneiss (*GR04036*) that cross-cuts a *Aqp*(±*Aqp*) unit on the northwest point of Case Study #1. As previously noted, quartz–pyroxene (*Aqp*) units found throughout the *Føringhavn terrane* are dominantly Qtz + Cpx (Hd) ± Opx (Fs).¹ The presence of the clinopyroxene hedenbergite (Morimoto, 1988) is common in high-grade regionally metamorphosed iron formations (eulysite; Deer et al., 1992) where the association with orthoferrosilite is stable (Lindsley, 1983). The *Aqp* units in this study possess Th/Sc, Cr/Th and Y/Cr values that are similar (but not identical) to the majority of Isua sediments, including BIF lithologies, and are different from mafic- to ultramafic igneous rocks (Fig. 17B).

Rare earth element patterns support a chemical sedimentary origin for the *Aqp* and *Aqp* units (Fig. 18). As reviewed elsewhere (Manning et al., 2006) local LREE mobility is a common feature of prograde metamorphic devolatilizations so that loss or gain of mobile LREE depending on degree of volatile loss makes the *Aqp* REE patterns of Akilia units (and those reported in this study) similar to less-altered Isua banded iron-formation. The REE patterns for samples *GR04041* and *GR04054* differ in general terms from Isua

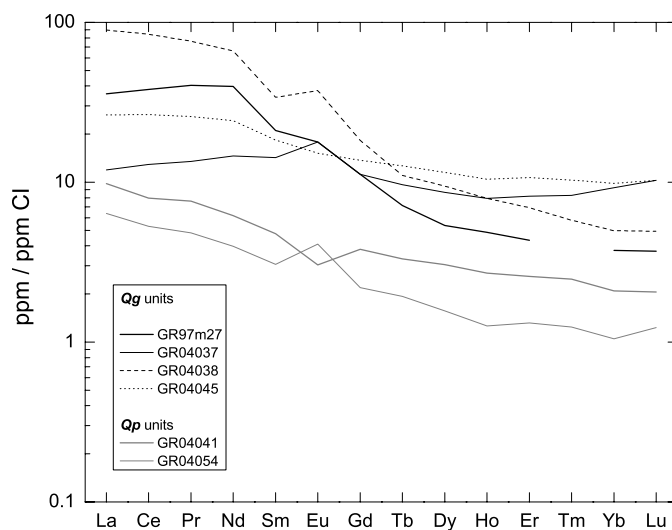


Fig. 18. REE diagram of samples with probable sedimentary origin from this study. Chondritic values from Anders and Grevesse (1989).

BIF and quartz–pyroxene/BIF rocks from Akilia (Fedo and Whitehouse, 2002a; Bolhar et al., 2004; Manning et al., 2006). Innersuartaq *Aqp* rocks are LREE enriched and most resemble Isua quartz–magnetite and Al-rich BIF facies even given the differences in metamorphic grade between the two terranes. Sample *GR04054* (*Aqp*) has a positive Eu anomaly, whereas *GR04041* is negative. As pointed out in Mojzsis and Harrison (2002b), Fedo and Whitehouse (2002b) and Manning et al. (2006), REE, and Eu in particular, can be significantly changed in metamorphism and should not be used exclusively as a measure of protolith type. If some information is retained, small differences in depositional settings and source (hydrothermal) fluids may explain the differences between the Akilia quartz–pyroxene units explored in Fedo and Whitehouse (2002a) and Manning et al. (2006), and those in this study. For example, the contemporary Lau and Manus back-arc basin sites (Western Pacific) yield hydrothermal vent fluids with concave up (and down) LREE patterns with (and without) Eu anomalies (Douville et al., 1999) which are quite similar to the patterns for our *Aqp* lithologies.

Bolhar and others (2004) proposed that a critical yardstick for the determination of sedimentary protolith (i.e., banded iron-formation or a generic marine sedimentary precipitate) is they contain superchondritic Y/Ho; chondritic values are 28.06 (Anders and Grevesse, 1989). Bolhar et al. (2004) advised using Y/Ho values above ~40 as a BIF discriminator. Our *Aqp* values are elevated with respect to chondritic (31.3–36; EA-1), which again is similar to units of this lithology found on Akilia (30–33), yet obviously below 40. However, if using the $Y/Ho \geq 40$ criterion of Bolhar et al. (2004) cited above, four of eight well-preserved laminated quartz–magnetite Isua BIF samples reported in their Table 2 have values below ~38, which highlights the ambiguity of using Y/Ho ratios as a protolith determinant.

Igneous rocks define a narrow range of Fe isotope values (Beard and Johnson, 2004); banded iron-formations

¹ Nomenclature of Kretz (1983).

and other marine sedimentary (chemical) precipitates that formed in the first half of Earth history have highly variable Fe isotopic compositions (Johnson et al., 2003) and can be used to infer protolith in Eoarchean rocks. Dauphas et al. (2004) have shown that Akilia meta-igneous units (*Au*, *Am*, *Aum*) have Fe isotope compositions similar to their modern equivalents. However, Akilia and Inner-suartuut quartz–pyroxene and banded ferruginous quartzites are enriched in the heavy isotope and have a definite BIF signature. The results of this study and that of Manning et al. (2006) are completely consistent with the report of Dauphas et al. (2004) that *Aqp* rocks are of sedimentary origin.

7.3. Multiple sulfur isotopes as a sedimentary protolith discriminator

The presence of MIF sulfur in our *Aqq*, *Aqp* and *Aqb* samples (Table 2) provides a powerful and mutually supportive means in concert with mineralogy, major-, minor- and trace-element grounds cited above, oxygen isotopes and Fe isotopes of Dauphas et al. (2004) for assigning a sedimentary protolith to highly metamorphosed rocks. We find that the *Aqp* units GR04041 and GR04054, banded iron-formation GR04063 and *Aqq* unit GR97m27 all contain mass-independently fractionated sulfur isotopes consistent with a sedimentary protolith.

7.4. Oxygen isotopes as a sedimentary protolith discriminator

Based on U–Pb isotopic compositions and correlative CL imagery with *in situ* zircon oxygen isotope compositions, zircons we investigated from the *Aqq* units are exclusively metamorphic in nature and formed in isotopic equilibrium with the paragneiss mineralogy of the rock. The oxygen isotopic composition of zircons extracted from candidate sediment *Aqq* (sample GR97m27) with ages up to ca. 3650 Ma yield an average value $+14.0 \pm 0.9\%$ (Table 4) which corresponds to a whole-rock value of $\sim +16.2\%$ assuming a zircon-rock oxygen isotope fractionation of $\sim +2.2\%$ (Zheng, 1993; Valley et al., 1994). This result is within error of the $\delta^{18}\text{O}_{\text{WR}}$ value for *Aqq* (+16.0%; Table 4) and agrees with other sedimentary units from West Greenland. Perry et al. (1978) reported data for Isua BIF $\delta^{18}\text{O}_{\text{WR}}$ of +12.9–20.4‰ and at Akilia, ferruginous quartz–pyroxene rocks have $\delta^{18}\text{O}_{\text{WR}}$ of +12.8–13.2‰ (Manning et al., 2006) within the range of values reported for Archean cherts (Knauth and Lowe, 2003). Our $\delta^{18}\text{O}_{\text{Zr}}$ from the quartz–garnet schists (*Aqq*) are in marked contrast to *Ag* units from Innersuurtuut which range from +6.1‰ to +8.3‰ (Table 4); these are values typical for Archean orthogneisses (Valley, 2003).

Results demonstrate that oxygen isotopic compositions of zircon support the interpretation of metamorphic vs. primary igneous vs. “inherited” grains based on U–Pb sys-

tematics, bulk composition of whole rock, zircon saturation temperatures and field relations.

7.5. Zircon growth and major geologic events in the Faeringhavn terrane

Zircon can grow *in situ* during prograde metamorphic recrystallization and isotopic resetting of the pre-existing grains (e.g., Ayers and Watson, 1991; Hoskin and Black, 2000) or via different zircon-forming reactions nurtured by intragranular melt/metasomatic fluids (e.g., Vavra et al., 1996; Rubatto et al., 2001; Hermann and Rubatto, 2003) from the breakdown of common Zr-bearing phases such as hornblende and garnet (Fraser et al., 1997). Metamorphic zircon growth in our samples is exemplified characterized by (i) weak to absent zoning in CL images (EA-5); (ii) low aspect ratio so that habit is commonly rounded to stubby; (iii) highly variable $[\text{Th}/\text{U}]_{\text{Zr}}$ inconsistent with Th + U partitioning between zircon and melt; (iv) turbid cores with clearer overgrowths or monotonous internal structures in transmitted light microscopy; and (v) markedly non-igneous $\delta^{18}\text{O}_{\text{Zr}}$ composition, sometimes characteristic of the whole grain in the case of purely metamorphic zircon, or correlative with discrete and younger metamorphic overgrowths on the original (igneous) cores.

7.5.1. Igneous zircons in TTG-type gneisses within supracrustal enclaves

In a recent study, Whitehouse and Kamber (2005) postulated that widespread inheritance of ancient zircon is the expected result for thin gneissic veins of TTG-type composition in polyphase metamorphic. To refute an age assignment of 3830 Ma to the tonalitic orthogneiss on Akilia (sample G93-05 of Nutman et al., 1997; sample GR9716 of Mojzsis and Harrison, 2002a), it was proposed that “partial melt of a ca. 3.84 Ga grey gneiss precursor at granulite facies with residual garnet” (Whitehouse and Kamber, 2005, p. 291) and migration of the tonalitic mush into the supracrustal rocks occurred at ~ 3650 Ma. However, these scenarios fail to explain how only a few specific granitoid sheets in the supracrustal enclaves are the exclusive means or the expected medium for selective zircon inheritance from an unknown supply of ancient zircons. Why for example, are the REE compositions of ca. 3650 Ma and younger zircons from the Akilia orthogneiss unit incompatible with any possible igneous compositions (Manning et al., 2006)? Instead, it makes sense to explore how the compositions of the various zircon populations compare with the expected compositions for igneous zircon growth in the bulk composition of the host rock.

Many small *Ag* sheets within or associated with supracrustals on Angisorssuaq (island) to the north and west of our study area (sample GGU110999 of Kinny, 1986) and several *Ag* units on Akilia (Nutman et al., 1997, 2000, 2002, 2004; Mojzsis and Harrison, 2002a; Manning et al., 2006) are also the oldest recognized components (>3810 Ma) in the Faeringhavn terrane. Although several

independent lines of evidence can be used to support a magmatic origin for the oldest *Ag* zircons captured in the supracrustals, the geochronological (degree of concordance), chemical (Th/U, REE) and isotopic ($\delta^{18}\text{O}_{\text{Zr}}$) characters cited above do not separately provide the “smoking gun” for an origin as emplaced magmas. Yet, taken together, these results provide a self-consistent scenario in which (older) volcano-sedimentary packages are gradually invaded by granitoid sheets as the supracrustal rocks become merged into developing batholiths (Petford, 1996; Wiebe et al., 2002; Coleman et al., 2004).

7.5.2. Tectonic emplacement of the oldest TTG-type gneisses in supracrustal enclaves

Except in exceptional circumstances, high degree of deformation precludes the preservation of conclusive cross-cutting contact relationships between *Ag* bodies and supracrustal units (such a *Aqp* and *Aqg*). However, comparison of the rock compositions and zircon age relations of the different units provides crucial clues to support a pre-3750 Ma of supracrustal enclaves in this study. If the geometries of the *Ag* bodies within the supracrustal rocks have a tectonic origin then it would be logical to expect a sample population of zircons with an average distribution of ages from the surrounding *IGC* rocks. Because this is not seen in the geochronology data, a tectonic emplacement origin as endorsed for the Akilia rocks in Myers and Crowley (2000) and Whitehouse and Fedo (2002), or hybrid meta-igneous origin of Whitehouse and Kamber (2005), must appeal to a special set of unique circumstances leading to preferential sampling of inherited (older) *Ag* zircon ages from some unspecified source that, coincidentally, happen to be the only components that are consonant with the bulk compositions of the host rocks.

7.5.3. Metamorphic zircon growth in Akilia association lithologies

The high-grade polyphase metamorphism that accompanied terrane assembly in the Ameralik region could result in multiple generations of growth on pre-existing zircon and/or wholesale growth of new zircon. Based on the criteria outlined above, we find that the oldest igneous zircon cores in this study are *ca.* 3770 Ma with other age populations extending to 1800 Ma. Results summarized in Table 1 show that major metamorphic zircon-growth events occurred at \sim 3650 Ma and at \sim 2700 Ma. These ages are to the same as those for regional granulite and amphibolite facies metamorphism recognized to have affected coastal outcrops of the *Faeringhavn terrane* beginning with the work of Black et al. (1971); McGregor (1973) and Griffin et al. (1980) and summarized in Nutman et al. (2004).

8. Conclusions

Concerns have been raised about whether primary intrasupracrustal lithologic relations such as original igneous contacts can be preserved in the face of the complex kine-

matic and thermal history of polymetamorphism in the southern *Itsaq Gneiss Complex*. Various competing and mutually exclusive hypotheses have been proposed for what constitutes evidence for sedimentary protolith in such rocks, and whether we can know the emplacement ages of various units. Integrated study leads to the identification of metasediments when coordinated with detailed maps to guide sample selection, high-resolution geochronology and stable isotope studies. It is possible that the various enclaves in the *IGC* embody a collective supracrustal “emulsion” of an autochthonous pre-3700 Ma terrane, fragmented and caught in a cross-section of Archean crust tectonically rotated and planed-off by erosion (*e.g.*, Pichamuthu, 1965). This was the original premise for the *Akilia association* offered by McGregor and Mason (1977). Alternatively, the *Akilia association* rocks on Akilia or Inner-suartuut may have originated as distinct entities, either older than other supracrustal packages in the *IGC* (Nutman et al., 1997), or perhaps younger than the *Isua supracrustal belt* (Myers and Crowley, 2000). If the origin of the *Akilia association* rocks cannot be reconciled with a shared parentage with Isua, then the *Itsaq Gneiss Complex* is an allochthonous terrane.

Mafic amphibolite gneiss units that volumetrically dominate the supracrustal enclaves reported here are broadly basaltic in composition and differ from Isua amphibolites in having LREE-enrichments, but retain negative Nb anomalies consistent with arc type tholeiitic magmas. Intercalated siliceous units such as ferruginous quartz–garnet biotite schists (*Aqg* and *Aqb*) compositionally resemble pelagic clays from weathering of mafic rocks. Quartz–pyroxene units (*Aqp*) appear to have a chemical affinity with the banded iron-formations as previously suggested by McGregor and Mason (1977) and bolstered by recent Fe isotope studies (Dauphas et al., 2004) and other geochemical analyses (Manning et al., 2006). Quartz–pyroxene rocks in particular resemble the Al- and quartz–magnetite facies BIF, with some important differences; trace element compositions match them more with derivation from back-arc basin hydrothermal fluid sources. No clear evidence is seen for input from any (proto?) continental source in these units and the rocks do not appear to carry detrital zircons. The association of *Aqp* with *Am* units with island-arc basaltic affinity suggests a depositional environment dominated by seafloor mafic volcanism and chemical sedimentation in an evolving plate margin setting before *ca.* 3750 Ma.

Metasedimentary *Aqg*, *Aqb* and *Aqp* units share complex metamorphic histories. They are cut by *ca.* 3750 Ma gneisses and contain zircon that grew during metamorphism at *ca.* 3650, 2700 Ma, and sometimes evidence is preserved for overprints from yet earlier events. Whole-rock oxygen isotope compositions of the sedimentary protoliths range from $\delta^{18}\text{O}_{\text{SMOW}}$ values of +13 to +17‰ and in the case of measured $\delta^{18}\text{O}_{\text{Zr}}$ values and Th/U, are consistent with growth of the zircons during high-grade metamorphism. Zircon oxygen isotope and U/Th compositions for grains extracted from metasedimentary candidate rocks

cannot be reconciled with an igneous origin and grew as a consequence of one or more metamorphic events. Mass-independently fractionated sulfur isotopes and ^{18}O -enriched oxygen in Aqp and Agg rocks are consistent with a low-temperature aqueous sediment source in the prevailing (anoxic) atmospheric conditions of the Archean. Therefore these rocks are relevant source materials to investigate conditions prevalent at the surface during the emergence of life. The approach presented here advocates integrating detailed mapping coupled with O- and S-isotopes studies, immobile trace elements and REE pattern discrimination, and geochronological techniques in the search for the oldest sediments. This methodology minimizes concerns regarding zircon inheritance and transcends different interpretations of the origin of supracrustal lithologies.

Acknowledgments

Technical assistance with the UCLA Cameca ims1270 ion microprobe from A. Schmitt, M. Grove and G. Jarzabinski is gratefully appreciated. We thank C.E. Manning and T.M. Harrison for many helpful discussions on this work, and C.E. Manning for original sketch map of Case Study 3. D. Papineau and D. Trail helped in the fieldwork, geochronology and stable isotope analyses. A.P. Nutman provided unpublished maps, and along with comments from two anonymous reviewers, helped to greatly improve the manuscript. We thank A. Brandon who helped shepherd this paper through the process. High-precision (and high-throughput) geochemical analyses by Marc Norman at ANU-PRISE, Phil Robinson at University of Tasmania and Georges Beaudouin at Université Laval (Québec) helped make this work possible. CL imaging was done by George Morgan and David London at the University of Oklahoma Electron Microprobe Laboratory. We thank Christian de Renouard and Boat Charter Hans Egede for providing transportation to field areas. This work was supported by the NASA Exobiology Program (NAG5-13497) to S.J.M. and a cooperative agreement between the NASA Astrobiology Institute and the CU Center for Astrobiology. Facility support to the UCLA ion microprobe center comes from the Instrumentation and Facilities Program of the National Science Foundation.

Associate editor: Alan D. Brandon

Appendix A. Supplementary data

Supplementary data associated with this article can be found, in the online version, at [doi:10.1016/j.gca.2006.05.014](https://doi.org/10.1016/j.gca.2006.05.014).

References

Anbar, A.D., Zahnle, K.J., Arnold, G.L., Mojzsis, S.J., 2001. Extraterrestrial iridium sediment accumulation and the habitability of the early Earth's surface. *J. Geophys. Res.* **106**, 3219–3236.

- Anders, E., Grevesse, N., 1989. Abundances of the elements—meteoric and solar. *Geochim. Cosmochim. Acta* **53**, 197–214.
- Ayers, J.C., Watson, E.B., 1991. Solubility of apatite, monazite, zircon and rutile in supercritical aqueous fluids with implications for subduction zone geochemistry. *Philos. Trans. R. Soc. Lond. Ser. A* **335**, 365–375.
- Ayers, J.C., De La Cruz, K., Miller, C., Switzer, O., 2003. Experimental study of zircon coarsening in quartzite +/- H₂O at 1.0 GPa and 1000 degrees C, with implications for geochronological studies of high-grade metamorphism. *Am. Mineral.* **88**, 365–376.
- Baadsgaard, H., Lambert, R.St J., Krupicka, J., 1976. Mineral isotopic age relationships in the polymetamorphic Amitsoq gneisses, Godthaab District, West Greenland. *Geochim. Cosmochim. Acta* **40**, 513–527.
- Baublys, K.A., Golding, S.D., Young, E., Kamber, B.S., 2004. Simultaneous determination of $\delta^{33}\text{Sv-CDT}$ and $\delta^{34}\text{Sv-CDT}$ using masses 48, 49 and 50 on a continuous flow isotope ratio mass spectrometer. *Rapid Commun. Mass Spectrom.* **18**, 2765–2769.
- Barker, F., 1979. Trondhjemite: definition, environment and hypotheses of origin. In: Barker, F. (Ed.), *Trondhjemites, Dacites, and Related Rocks*. Elsevier, Amsterdam, pp. 1–12.
- Beard, B.L., Johnson, C.M., 2004. Fe isotope variations in the modern and ancient earth and other planetary bodies. *Rev. Min. Geochem.* **55**, 319–357.
- Bekker, A., Holland, H.D., Wang, P.-L., Rumble III, D., Stein, H.J., Hannah, J.L., Coetzee, L.L., Beukes, N.J., 2004. Dating the rise of atmospheric oxygen. *Nature* **427**, 117–120.
- Bennett, V.C., Nutman, A.P., Esat, T.M., 2002. Constraints on mantle evolution from $^{187}\text{Os}/^{188}\text{Os}$ isotopic compositions of Archean ultramafic rocks from southern West Greenland (3.8 Ga) and Western Australia (3.46 Ga). *Geochim. Cosmochim. Acta* **66**, 2615–2630.
- Black, L.P., Gale, N.H., Moorbath, S., Pankhurst, R.J., McGregor, V.R., 1971. Isotopic Dating of very early Precambrian amphibolite facies gneisses from Godthaab district, West Greenland—Oxford Isotope Geology Laboratory. *Earth Planet. Sci. Lett.* **12**, 245.
- Black, L.P., Kamo, S.L., Williams, I.S., Mundil, R., Davis, D.W., Korsch, R.J., Foudoulis, C., 2003. The application of SHRIMP to Phanerozoic geochronology; a critical appraisal of four zircon standards. *Chem. Geol.* **200**, 171–188.
- Bleeker, W., 2004. Towards a 'natural' time scale for the Precambrian—a proposal. *Lethaia* **37**, 219–222.
- Bolhar, R., Kamber, B.S., Moorbath, S., Fedo, C.M., Whitehouse, M.J., 2004. Characterisation of early Archaean chemical sediments by trace element signatures. *Earth Planet. Sci. Lett.* **222**, 43–60.
- Bolhar, R., Kamber, B.S., Moorbath, S., Whitehouse, M.J., Collerson, K.D., 2005. Chemical characterization of earth's most ancient clastic metasediments from the Isua Greenstone Belt, southern West Greenland. *Geochim. Cosmochim. Acta* **69**, 1555–1573.
- Bottinga, Y., Javoy, M., 1975. Oxygen isotope partitioning among minerals in igneous and metamorphic rocks. *Rev. Geophys.* **13**, 401–418.
- Bridgwater, D., McGregor, V.R., 1974. Field work on the very early Precambrian rocks of the Isua area, southern west Greenland. *Rapp. Grønlands Geol. Unders.* **65**, 49–54.
- Carmichael, R.S. (Ed.), 1989. *Practical Handbook of Physical Properties of Rocks and Minerals*. CRC Press, Boca Raton, FL, p. 714.
- Cates, N.L., Mojzsis, S.J., 2006. Geochronology and geochemistry of a newly identified pre-3760 Ma supracrustal sequence in the Nuvvuagittuq belt, Québec, Canada. *Lunar Planet. Sci.* **37**, #1948 (abstr.).
- Cavosie, A.J., Valley, J.W., Wilde, S.A., E.I.M.F., 2005. Magmatic $\delta^{18}\text{O}$ in 4400–3900 Ma detrital zircons: a record of the alteration and recycling of crust in the Early Archean. *Earth Planet. Sci. Lett.* **235**, 663–681.
- Chadwick, B., Coe, K., 1983. Geological map of Greenland, 1:100,000, Buksefjorden. *Grønlands Geol. Unders.* 63 Denmark, p. 70.
- Chadwick, B., Coe, K., 1984. Archaean crustal evolution in southern West Greenland; a review based on observations in the Buksefjorden region. *Tectonophysics* **105**, 121–130.
- Coleman, D.S., Gray, W., Glazner, A.F., 2004. Rethinking the emplacement and evolution of zoned plutons; geochronologic evidence for

- incremental assembly of the Tuolumne Intrusive Suite, California. *Geology* **32**, 433–436.
- Dauphas, N., van Zuilen, M., Wadhwa, M., Davis, A.M., Marty, B., Janney, P.E., 2004. Geochemistry: clues from Fe isotope variations on the origin of Early Archean BIFs from Greenland. *Science* **306**, 2077–2080.
- Deer, W.A., Howie, R.A., Zussman, J., 1992. *An Introduction to the Rock-forming Minerals*. Longman Scientific Technical, UK.
- Douville, E., Bienvu, P., Charlou, J.L., Donval, J.P., Fouquet, Y., Appriou, P., Gamo, T., 1999. Yttrium and rare earth elements in fluids from various deep-sea hydrothermal systems. *Geochim. Cosmochim. Acta* **63**, 627–643.
- Dymek, R.F., Klein, C., 1988. Chemistry, petrology and origin of banded iron-formation lithologies from the 3800 Ma Isua supracrustal belt, West Greenland. *Precamb. Res.* **39**, 247–302.
- Farquhar, J., Wing, B.A., 2003. Multiple sulfur isotopes and the evolution of the atmosphere. *Earth Planet. Sci. Lett.* **213**, 1–13.
- Farquhar, J., Bao, H.M., Thiemens, M., 2000. Atmospheric influence of Earth's earliest sulfur cycle. *Science* **289**, 756–758.
- Fedo, C.M., Whitehouse, M.J., 2002a. Metasomatic origin of quartz–pyroxene rock, Akilia, Greenland and implications for Earth's earliest life. *Science* **296**, 1448–1452.
- Fedo, C.M., Whitehouse, M.J., 2002b. Origin and significance of Archean quartzose rocks at Akilia, Greenland—Response. *Science* **298**, 917a.
- Fedo, C.M., Myers, J.S., Appel, P.W.U., 2001. Depositional setting and paleogeographic implications of earth's oldest supracrustal rocks, the >3.7 Ga Isua Greenstone belt, West Greenland. *Sediment. Geol.* **141**, 61–77.
- Fraser, G., Ellis, D., Eggins, S., 1997. Zirconium abundance in granulite-facies minerals, with implications for zircon geochronology in high-grade rocks. *Geology* **25**, 607–610.
- Frei, R., Rosing, M.T., Waight, T.E., Ulfbeck, D.G., 2002. Hydrothermal-metasomatic and tectono-metamorphic processes in the Isua supracrustal belt (West Greenland): a multi-isotopic investigation of their effects on the Earth's oldest oceanic crustal sequence. *Geochim. Cosmochim. Acta* **66**, 467–486.
- Friend, C.R.L., Nutman, A.P., 2005a. Complex 3670–3500 Ma orogenic episodes superimposed on juvenile crust accreted between 3850 and 3690 Ma, Itsaq Gneiss Complex, Southern West Greenland. *J. Geol.* **113**, 375–397.
- Friend, C.R.L., Nutman, A.P., 2005b. New pieces to the Archean terrane jigsaw puzzle in the Nuuk region, southern West Greenland: steps in transforming a simple insight into a complex regional tectonothermal model. *J. Geol. Soc.* **162**, 147–162.
- Friend, C.R.L., Nutman, A.P., Baadsgaard, H., Kinny, P.D., McGregor, V.R., 1996. Timing of late Archean terrane assembly, crustal thickening and granite emplacement in the Nuuk region, southern West Greenland. *Earth Planet. Sci. Lett.* **142**, 353–365.
- Friend, C.R.L., Nutman, A.P., Bennett, V.C., 2002a. Protoliths of the 3.8–3.7 Ga Isua greenstone belt: discussion. *Precamb. Res.* **117**, 145–149.
- Friend, C.R.L., Bennett, V.C., Nutman, A.P., 2002b. Abyssal peridotites >3,800 Ma from southern West Greenland; field relationships, petrography, geochronology, whole-rock and mineral chemistry of dunite and harzburgite inclusions in the Itsaq Gneiss Complex. *Contrib. Miner. Petrol.* **143**, 71–92.
- Gancarz, A.J., Wasserberg, G.J., 1977. Initial Pb of the Amitsoq Gneiss, West Greenland and implications for the age of the Earth. *Geochim. Cosmochim. Acta* **41**, 1283–1301.
- Greenwood, J.P., Mojzsis, S.J., Coath, C.D., 2000. Sulfur isotopic compositions of individual sulfides in Martian meteorites ALH84001 and Nakhla; implications for crust–regolith exchange on Mars. *Earth Planet. Sci. Lett.* **184**, 23–35.
- Griffin, W.L., McGregor, V.R., Nutman, A.P., Taylor, P.N., Bridgwater, D., 1980. Early Archean granulite-facies metamorphism south of Ameralik, West Greenland. *Earth Planet. Sci. Lett.* **50**, 59–74.
- Gruau, G., Nutman, A., Jahn, B.M., 1986. Significance of the Sm–Nd isotopic systematics of the Akilia Association. *LPI Technical Report* **86**, 55–58.
- Harrison, T.M., Watson, E.B., 1983. Kinetics of zircon dissolution and zirconium diffusion in granitic melts of variable water content. *Contrib. Miner. Petrol.* **84**, 66–72.
- Harrison, T.M., Bichert-Toft, J., Müller, W., Albarède, F., Holden, P., Mojzsis, S.J., 2005. Heterogeneous Hadean hafnium: evidence of significant continental crust at 4.4 to 4.5 Ga. *Science* **310**, 1947–1950.
- Hermann, J., Rubatto, D., 2003. Relating zircon and monazite domains to garnet growth zones: age and duration of granulite facies metamorphism in the Val Malenco lower crust. *J. Metamorph. Geol.* **21**, 833–852.
- Hoskin, P.W.O., Black, L.P., 2000. Metamorphic zircon formation by solid-state recrystallization of protolith igneous zircon. *J. Metamorph. Geol.* **18**, 423–439.
- Hoskin, P.W.O., Schaltegger, U., 2003. The composition of zircon and igneous and metamorphic petrogenesis. *Rev. Min. Geochem.* **53**, 27–62.
- Irvine, T.N., Baragar, W.R.A., 1971. A guide to the chemical classification of common volcanic rocks. *Can. J. Earth Sci.* **8**, 523–548.
- Johnson, C.M., Beard, B.L., Beukes, N.J., Klein, C., O'Leary, J.M., 2003. Ancient geochemical cycling in the Earth as inferred from Fe isotope studies of banded iron formations from the Transvaal Craton. *Contrib. Miner. Petrol.* **144**, 523–547.
- Kamber, B.S., Moorbath, S., 2000. Initial Pb of the Amitsoq Gneiss revisited: implications for the timing of early Archean crustal evolution in West Greenland: reply. *Chem. Geol.* **166**, 309–312.
- Kamber, B.S., Collerson, K.D., Moorbath, S., Whitehouse, M.J., 2003. Inheritance of early Archean Pb-isotope variability from long-lived Hadean protocrust. *Contrib. Miner. Petrol.* **145**, 25–46.
- Kinny, P.D., 1986. 3820 Ma zircons from a tonalitic Amitsoq Gneiss in the Godthaab District of southern West Greenland. *Earth Planet. Sci. Lett.* **79**, 337–347.
- Knauth, L.P., Lowe, D.R., 2003. High Archean climatic temperature inferred from oxygen isotope geochemistry of cherts in the 3.5 Ga Swaziland Supergroup, South Africa. *Geol. Soc. Am. Bull.* **115**, 566–580.
- Komiya, T., Maruyama, S., Masuda, T., Nohda, S., Hayashi, M., Okamoto, K., 1999. Plate tectonics at 3.8–3.7 Ga; field evidence from the Isua accretionary complex, southern West Greenland. *J. Geol.* **107**, 515–554.
- Kretz, R., 1983. Symbols for rock-forming minerals. *Am. Mineral.* **68**, 277–279.
- Krogh, T.E., Kamo, S.L., Kwok, Y.Y., 2002. An isotope dilution, etch abrasion solution to the Akilia Island U–Pb age controversy. *Geochim. Cosmochim. Acta* **66**, A419 (abstr.).
- Lepland, A., van Zuilen, M.A., Arrhenius, G., Whitehouse, M.J., Fedo, C.M., 2005. Questioning the evidence for Earth's earliest life; Akilia revisited. *Geology* **33**, 77–79.
- Lindsley, D.H., 1983. Pyroxene thermometry. *Am. Mineral.* **68**, 477–493.
- Lowe, D.R., Byerly, G.R., 1999. Stratigraphy of the west-central part of the Barberton Greenstone Belt, South Africa. In Lowe, D.R., Byerly, G.R. (Eds.), *Geologic evolution of the Barberton Greenstone Belt, South Africa*. Geol. Soc. Am. Sp. Paper, vol. 329. pp. 1–36.
- Ludwig, K.R., 2001. User's manual for Isoplot/Ex rev. 2.49: A Geochronological Toolkit for Microsoft Excel. Berkeley Geochronological Center Special Publication 1a.
- Manning, C.E., Mojzsis, S.J., Harrison, T.M., 2006. Geology, age and origin of supracrustal rocks, Akilia, west Greenland. *Am. J. Sci.* **306**, 303–366.
- Maruyama, S., Masuda, S., Appel, P.W.U., 1991. The oldest accretionary complex on the Earth, Isua, Greenland. *Geol. Soc. Am. Abs. Prog.* **23**, A429–A430 (abstr.).
- McDonough, W., Sun, S., Ringwood, A.E., Jagoutz, E., Hofmann, A.W., 1992. Potassium, rubidium and cesium in the Earth and Moon and the evolution of the mantle of the Earth. *Geochim. Cosmochim. Acta* **56**, 1001–1012.
- McGregor, V.R., 1968. Field evidence of very old Precambrian rocks in the Godthåb area, West Greenland. *Rapp. Grønlands Geol. Unders.* **15**, 31–35.
- McGregor, V.R., 1973. The early Precambrian gneisses of the Godthåb district, West Greenland. *Philos. Trans. R. Soc. Lond.* **A237**, 343–358.

- McGregor, V.R., 1979. Archean gray gneisses and the origin of the continental crust; evidence from the Godthaab region, West Greenland. In: Barker, F. (Ed.), *Trondhjemites, Dacites, and Related Rocks*. Elsevier, Amsterdam, pp. 169–204.
- McGregor, V.R., 2000. Initial Pb of the Amitsoq gneiss revisited: implications for the timing of early Archean crustal evolution in West Greenland—Comment. *Chem. Geol.* **166**, 301–308.
- McGregor, V.R., Mason, B., 1977. Petrogenesis and geochemistry of metabasaltic and metasedimentary enclaves in the Amitsoq gneisses, West Greenland. *Am. Mineral.* **62**, 887–904.
- McLennan, S.M., Taylor, S.R., McGregor, V.R., 1984. Geochemistry of Archean meta-sedimentary rocks from West Greenland. *Geochim. Cosmochim. Acta* **48**, 1–13.
- Mojzsis, S.J., Harrison, T.M., 2000. Vestiges of a beginning: clues to the emergent biosphere recorded in the oldest known sedimentary rocks. *GSA Today* **10**, 1–6.
- Mojzsis, S.J., Harrison, T.M., 2002a. Establishment of a 3.83-Ga magmatic age for the Akilia tonalite (southern West Greenland). *Earth Planet. Sci. Lett.* **202**, 563–576.
- Mojzsis, S.J., Harrison, T.M., 2002b. Origin and significance of Archean quartzose rocks at Akilia, Greenland. *Science* **298**, 917.
- Mojzsis, S.J., Arrhenius, G., McKeegan, K.D., Harrison, T.M., Nutman, A.P., Friend, C.R.L., 1996. Evidence for life on Earth before 3,800 million years ago. *Nature* **384**, 55–59.
- Mojzsis, S.J., Harrison, T.M., Pidgeon, R.T., 2001. Oxygen-isotope evidence from ancient zircons for liquid water at the Earth's surface 4,300 Myr ago. *Nature* **409**, 178–181.
- Mojzsis, S.J., Coath, C.D., Greenwood, J.P., McKeegan, K.D., Harrison, T.M., 2003a. Mass-independent isotope effects in Archean (2.5 to 3.8 Ga) sedimentary sulfides determined by ion microprobe analysis. *Geochim. Cosmochim. Acta* **67**, 1635–1658.
- Mojzsis, S.J., Devaraju, T.C., Newton, R.C., 2003b. Ion microprobe U–Pb age determinations on zircon from the late Archean granulite facies transition zone of southern India. *J. Geol.* **111**, 407–425.
- Moorbath, S., 2005a. Palaeobiology—dating earliest life. *Nature* **434**, 155.
- Moorbath, S., 2005b. Oldest rocks, earliest life, heaviest impacts and the Hadean-Archean transition. *Appl. Geochem.* **20**, 819–824.
- Moorbath, S., Onions, R.K., Pankrust, R.J., 1973. Early Archean age for Isua iron formation, West Greenland. *Nature* **245**, 138–139.
- Moorbath, S., Whitehouse, M.J., Kamber, B.S., 1997. Extreme Nd-isotope heterogeneity in the early Archean; fact or fiction? Case histories from northern Canada and West Greenland. *Chem. Geol.* **135**, 213–231.
- Morimoto, N., 1988. Nomenclature of Pyroxenes. *Miner. Petrol.* **39**, 55–76.
- Myers, J.S., 2001. Protoliths of the 3.8–3.7 Ga Isua greenstone belt, West Greenland. *Precamb. Res.* **105**, 129–141.
- Myers, J.S., Crowley, J.L., 2000. Vestiges of life of life in the oldest Greenland rocks? A review of early Archean geology in the Godthåbsfjord region, and reappraisal of field evidence for >3850 Ma life on Akilia. *Precamb. Res.* **103**, 101–124.
- Nishizawa, M., Takahata, N., Terada, K., Komiya, T., Ueno, Y., Sano, Y., 2005. Rare-earth element, lead, carbon and nitrogen geochemistry of apatite-bearing metasediments from the ~3.8 Ga Isua Supracrustal Belt, West Greenland. *Int. Geol. Rev.* **47**, 952–970.
- Nutman, A.P., 1977. Geologic map of Southwest Greenland, unpublished.
- Nutman, A.P., 1984. Early Archean crustal evolution of the Isukasia area, southern West Greenland. In: Kröner, A., Greiling, R. (Eds.), *Precambrian Tectonics Illustrated*. E. Schweizerbart'sche Verlagsbuchhandlung, Stuttgart, pp. 76–94.
- Nutman, A.P., Friend, C.R.L., Kinny, P.D., McGregor, V.R., 1993. Anatomy of an early Archean gneiss complex; 3900 to 3600 Ma crustal evolution in southern West Greenland. *Geology* **21**, 415–418.
- Nutman, A.P., McGregor, V.R., Friend, C.R.L., Bennett, V.C., Kinny, P.D., 1996. The Itsaq Gneiss Complex of southern West Greenland; the world's most extensive record of early crustal evolution (2900–2600 Ma). *Precamb. Res.* **78**, 1–39.
- Nutman, A.P., Mojzsis, S.J., Friend, C.R.L., 1997. Recognition of ≥ 3850 Ma water-lain sediments in West Greenland and their significance for the early Archean Earth. *Geochim. Cosmochim. Acta* **61**, 2475–2484.
- Nutman, A.P., Bennett, V.C., Friend, C.R.L., Norman, M.D., 1999. Meta-igneous (non-gneissic) tonalites and quartzdiorites from an extensive ca. 3800 Ma terrain south of the Isua supracrustal belt, southern West Greenland; constraints on early crust formation. *Contrib. Miner. Petrol.* **137**, 364–388.
- Nutman, A.P., Friend, C.R.L., Bennett, V.C., McGregor, V.R., 2000. The early Archean Itsaq Gneiss Complex of southern West Greenland: the importance of field observations in interpreting dates and isotopic data constraining early terrestrial evolution. *Geochim. Cosmochim. Acta* **64**, 3035–3060.
- Nutman, A.P., McGregor, V.R., Shiraishi, K., Friend, C.R.L., Bennett, V.C., Kinny, P.D., 2002. > or =3850 Ma BIF and mafic inclusions in the early Archean Itsaq gneiss complex around Akilia, southern West Greenland? The difficulties of precise dating of zircon-free protoliths in migmatites. *Precamb. Res.* **117**, 185–224.
- Nutman, A.P., Friend, C.R.L., Barker, S.L.L., McGregor, V.R., 2004. Inventory and assessment of Paleoarchean gneiss terrains and detrital zircons in southern West Greenland. *Precamb. Res.* **135**, 281–314.
- Ohmoto, H., 1986. Stable isotope geochemistry of ore deposits. *Rev. Min. Geochem.* **16**, 491–559.
- Paces, J.B., Miller Jr., J.D., 1993. Precise U–Pb ages of Duluth Complex and related mafic intrusions, northeastern Minnesota; geochronological insights to physical, petrogenetic, paleomagnetic, and tectonometric processes associated with the 1.1 Ga Midcontinent Rift System. *J. Geophys. Res.* **B 98**, 13,997–14,013.
- Palin, J.M., 2002. The origin of a most contentious rock. *Science* **298**, 961.
- Pankhurst, R.J., Moorbath, S., McGregor, V.R., 1973. Late event in the geological evolution of the Godthaab District, West Greenland. *Nature* **243**, 24–26.
- Papineau, D., Mojzsis, S.J., Coath, C.D., Karhu, J.A., McKeegan, K.D., 2005. Multiple sulfur isotope analyses of sulfides in the aftermath of Paleoproterozoic glaciations. *Geochim. Cosmochim. Acta* **69**, 5033–5060.
- Pavlov, A.A., Kasting, J.F., 2002. Mass-independent fractionation of sulfur isotopes in Archean sediments: strong evidence for an anoxic Archean atmosphere. *Astrobiology* **2**, 27–41.
- Pearce, J.A., 1983. Role of the subcontinental lithosphere in magma genesis at active continental margins. In: Hawkesworth, C.J., Norry, M.J. (Eds.), *Continental Basalts and Mantle Xenoliths*. Shiva, Nantwich, pp. 230–249.
- Pearce, J.A., Cann, J.R., 1973. Tectonic setting of basic volcanic rocks determined using trace element analyses. *Earth Planet. Sci. Lett.* **19**, 290–300.
- Perry, E.C., Ahmad, S.N., Swilius, T.M., 1978. The oxygen isotope composition of 3800 m.y. old metamorphosed chert and iron formation from Isukasia, West Greenland. *J. Geol.* **86**, 223–239.
- Petford, N., 1996. Dykes or diapirs? *Trans. R. Soc. Edinb. Earth Sci.* **87**, 105–114.
- Pichamuthu, C.S., 1965. Regional metamorphism and charnockitization in Mysore State, India. *India Mineral.* **6**, 119–126.
- Polat, A., Hofmann, A.W., 2003. Alteration and geochemical patterns in the 3.7–3.8 Ga Isua greenstone belt, West Greenland. *Precamb. Res.* **126**, 197–218.
- Polat, A., Kerrich, R., 2001. Magnesian andesites, Nb-enriched basalt-andesites, and adakites from late-Archean 2.7 Ga Wawa greenstone belts, Superior Province, Canada: implications for late Archean subduction zone petrogenetic processes. *Contrib. Miner. Petrol.* **141**, 36–52.
- Polat, A., Hofmann, A.W., Rosing, M.T., 2002. Boninite-like volcanic rocks in the 3.7–3.8 Ga Isua greenstone belt, West Greenland: geochemical evidence for intra-oceanic subduction zone processes in the early Earth. *Chem. Geol.* **184**, 231–254.
- Polat, A., Hofmann, A.W., Münker, C., Regelous, M., Appel, P.W.U., 2003. Contrasting geochemical patterns in the 3.7–3.8 Ga pillow basalt cores and rims, Isua greenstone belt, Southwest Greenland: implications for postmagmatic alteration processes. *Geochim. Cosmochim. Acta* **67**, 441–457.

- Rollinson, H., 2001. Searching for the earliest record of life on Earth. *Geol. Today* **17**, 180–185.
- Rose, N.M., Rosing, M.T., Bridgwater, D., 1996. The origin of metacarbonate rocks in the Archaean Isua supracrustal belt, West Greenland. *Am. J. Sci.* **296**, 1004–1044.
- Rosing, M.T., 1999. C-13-depleted carbon microparticles in >3700-Ma sea-floor sedimentary rocks from West Greenland. *Science* **283**, 674–676.
- Rosing, M.T., Rose, N.M., Bridgwater, D., Thomsen, H.S., 1996. Earliest part of Earth's stratigraphic record: A reappraisal of the >3.7 Ga Isua (Greenland) supracrustal sequence. *Geology* **24**, 43–46.
- Rubatto, D., Williams, I.S., Buick, I.S., 2001. Zircon and monazite response to prograde metamorphism in the Reynolds Range, central Australia. *Contrib. Miner. Petrol.* **140**, 458–468.
- Schidlowski, M., 1988. A 3,800-million-year isotopic record of life from carbon in sedimentary rocks. *Nature* **333**, 313–318.
- Schidlowski, M., Appel, P.W.U., Eichmann, R., Junge, C.E., 1979. Carbon isotope geochemistry of the 3.7×10^9 yr old Isua sediments, West Greenland; implications for the Archaean carbon and oxygen cycles. *Geochim. Cosmochim. Acta* **43**, 189–200.
- Schuhmacher, M., de Chambost, E., McKeegan, K.D., Harrison, T.M., Migeon, H., 1994. Dating of zircon with the CAMECA IMS 1270. In: Benninghoven, A., Nihei, Y., Shimizu, R., Werner, H.W. (Eds.), *Secondary Ion Mass Spectrometry SIMS IX*. Wiley, New York, pp. 912–922.
- Streckeisen, A., 1976. To each plutonic rock its proper name. *Earth Sci. Rev.* **12**, 1–33.
- Turner, G., Harrison, T.M., Holland, G., Mojzsis, S.J., Gilmour, J., 2004. Extinct Pu-244 in ancient zircons. *Science* **306**, 89–91.
- Ueno, Y., Yurimoto, H., Yoshioka, H., Komiya, T., Maruyama, S., 2002. Ion microprobe analysis of graphite from ca. 3.8 Ga metasediments, Isua supracrustal belt, West Greenland; relationship between metamorphism and carbon isotopic composition. *Geochim. Cosmochim. Acta* **66**, 1257–1268.
- Valley, J.W., 2003. Oxygen isotopes in zircon. In: Hanchar, J.M., Hoskin, P.W. (Eds.), *Reviews in Mineralogy and Geochemistry*, vol. 53. Mineralogical Society of America and Geochemical Society, Washington, DC, pp. 343–385.
- Valley, J.W., Chiarenzelli, J.R., McLelland, J.M., 1994. Oxygen-isotope geochemistry of zircon. *Earth Planet. Sci. Lett.* **126**, 187–206.
- Valley, J.W., Bindeman, I.N., Peck, W.H., 2003. Empirical calibration of oxygen isotope fractionation in zircon. *Geochim. Cosmochim. Acta* **67**, 3257–3266.
- Van Zuilen, M., Lepland, A., Arrhenius, G., 2002. Reassessing the evidence for the earliest traces of life. *Nature* **418**, 627–630.
- Vavra, G., Gebauer, D., Schmid, R., Compston, W., 1996. Multiple zircon growth and recrystallization during polyphase Late Carboniferous to Triassic metamorphism in granulites of the Ivrea Zone (Southern Alps): an ion microprobe (SHRIMP) study. *Contrib. Miner. Petrol.* **122**, 337–358.
- Watson, E.B., 1996. Dissolution, growth and survival of zircons during crustal fusion: kinetic principles, geologic models and implications for isotopic inheritance. *Proc. R. Soc. Edinb.* **87**, 43–56.
- Watson, E.B., Cherniak, D.J., 1997. Oxygen diffusion in zircon. *Earth Planet. Sci. Lett.* **148**, 527–544.
- Wiebe, R.A., Blair, K.D., Hawkins, D.P., Sabine, C.P., 2002. Mafic injections, in situ hybridization, and crystal accumulation in the Pyramid Peak granite, California. *Geol. Soc. Am. Bull.* **114**, 909–920.
- Whitehouse, M.J., Fedo, C.M., 2002. Early Archean life-bearing ocean or shear zone? Akilia re-evaluated. *Geochim. Cosmochim. Acta* **66**, 833.
- Whitehouse, M.J., Fedo, C.M., 2003. Deformation features and critical field relationships of early Archean rocks, Akilia, southwest Greenland. *Precamb. Res.* **126**, 259–271.
- Whitehouse, M.J., Kamber, B.S., 2005. Assigning dates to thin gneissic veins in high-grade metamorphic terranes: a cautionary tale from Akilia, southwest Greenland. *J. Petrol.* **46**, 291–318.
- Whitehouse, M., Kamber, B.S., Moorbath, S., 1999. Age significance of ion-microprobe U–Pb zircon data from early Archean rocks of West Greenland—a reassessment based on new combined ion-microprobe and imaging studies. *Chem. Geol.* **160**, 204–221.
- Whitehouse, M., Kamber, B.S., Fedo, C.M., Lepland, A., 2005. Integrated Pb- and S-isotope investigation of sulphide minerals from the early Archean of southwest Greenland. *Chem. Geol.* **222**, 112–131.
- Wyllie, P.J., Wolf, M.B., van der Laan, S.R., 1997. Conditions for formation of tonalites and trondhjemites: magmatic sources and products. In: de Wit, M.J., Ashwal, L.D. (Eds.), *Greenstone Belts*. Oxford University Press, Oxford, pp. 256–266.
- Zheng, Y.F., 1993. Calculation of oxygen isotope fractionation in anhydrous silicate minerals. *Geochim. Cosmochim. Acta* **57**, 1079–1091.